



## **IMPRESSIONS climate scenarios**

### **Deliverable D2.3**

September 2016

Marianne Sloth Madsen<sup>1</sup>, Cathrine Fox Maule<sup>1</sup>, Jens Hesselbjerg Christensen<sup>1</sup>,  
Stefan Fronzek<sup>2</sup> and Tim Carter<sup>2</sup>

<sup>1</sup>*Danish Meteorological Institute (DMI)*

<sup>2</sup>*Finnish Environment Institute (SYKE), Finland*



---

**Prepared under contract from the European Commission**

Contract n° 603416  
Collaborative project  
FP7 Environment

Project acronym: **IMPRESSIONS**  
Project full title: **Impacts and Risks from High-end Scenarios: Strategies for Innovative Solutions**  
Start of the project: 01 November 2013  
Duration: 60 months  
Project coordinator: NERC Centre for Ecology and Hydrology  
Project website: [www.impressions-project.eu](http://www.impressions-project.eu)

Deliverable title: IMPRESSIONS climate scenarios for all case studies  
Deliverable n°: D2.3  
Nature of the deliverable: Report  
Dissemination level: Public

WP responsible: WP2  
Lead beneficiary: Danish Meteorological Institute

Citation: Madsen, M.S., Maule, C.F., Christensen, J.H., Fronzek, S. & Carter, T.R. (2016). IMPRESSIONS Climate Scenarios. EU FP7 IMPRESSIONS Project Deliverable D2.3.

Due date of deliverable: Month n° 35  
Actual submission date: Month n° 35

The content of this deliverable do not necessarily reflect the official opinions of the European Commission or other institutions of the European Union.

## Table of contents

1. Introduction .....	5
2. Bias-adjustment of climate scenario data .....	6
2.1. Bias-adjustment methods .....	8
2.1.1. Delta Change .....	9
2.1.2. Quantile mapping.....	9
2.2. The WATCH WFDEI baseline data .....	12
3. Climate change projections .....	15
3.1. Bias-adjusted RCM data .....	15
3.2. Bias-adjusted GCM data.....	29
3.3. Comparison of RCM and GCM climate change .....	37
4. Climate indices for Europe.....	41
4.1. Customized data for the local case studies.....	47
4.1.1. Standardized Precipitation Index for the Iberian case study .....	47
4.1.2. Heat index for Hungary .....	48
4.1.3. Climate analogues for Scotland .....	52
5. Introduction to probabilistic climate scenarios .....	52
6. Acknowledgements.....	53
7. References .....	53

## Preface

In this Deliverable the climate scenarios selected for IMPRESSIONS are presented. The selection procedure was described in Deliverable D2.1 ‘Evaluation of existing climate and socio-economic scenarios including a detailed description of the final selection’ and only briefly summarized below. The present deliverable reports on activities related to Task 2.3: Climate Scenarios: new simulations, downscaling and analysis. The new IMPRESSIONS socio-economic scenarios are described separately in Deliverable 2.2.

The IMPRESSIONS climate scenarios were selected with a focus on high-end scenarios. The aim was primarily to portray the full range of climate sensitivity in the CMIP5 archive as far as possible and at the same time represent changes in global mean temperature from approximately 2°C to more than 4°C. Further to this, an important second constraint was imposed; in order to benefit from higher resolution simulations for the local and regional case studies, only GCMs that have been dynamically downscaled in CORDEX<sup>1</sup> were selected. The core set of GCM-RCMs used throughout the project is shown in Table 1.

**Table 1: Details of the core set of climate scenarios selected in IMPRESSIONS.**

Climate change	Emission scenario	GCM	RCM	GCM sensitivity
High	RCP8.5	HadGEM2-ES	RCA4	High
High	RCP8.5	CanESM2	CanRCM4	High
High	RCP8.5	IPSL-CM5A-MR	WRF	High
Intermediate	RCP8.5	GFDL-ESM2M	RCA4	Low
Intermediate	RCP4.5	HadGEM2-ES	RCA4	High
Low	RCP4.5	GFDL-ESM2M	RCA4	Low
Low	RCP4.5	MPI-ESM-LR	CCLM4	Low

The full model names are given below. These include the acronyms of the institutions that made the GCM/RCM simulation (e.g. MOHC and SMHI) and the specific number of the selected GCM realization (r1i1p1). We include only EUR-44-simulations with a resolution of ~50 km.

EUR-44-MOHC-HadGEM2-ES\_r1i1p1\_SMHI-RCA4\_v1 -> **HadGEM2-ES\_RCA4**  
 EUR-44-CCCma-CanESM2\_r1i1p1\_CCCma-CanRCM4\_r2 -> **CanESM2\_CanRCM4**  
 EUR-44-IPSL-IPSL-CM5A-MR\_r1i1p1\_IPSL\_INERIS-WRF331F\_v1 -> **IPSL-CM5A-MR\_WRF**  
 EUR-44-NOAA-GFDL-GFDL\_ESM2M\_r1i1p1\_SMHI\_RCA4\_v1 -> **GFDL-ESM2M\_RCA4**  
 EUR-44-MOHC-HadGEM2-ES\_r1i1p1\_SMHI-RCA4\_v1 -> **HadGEM2-ES\_RCA4**  
 EUR-44-NOAA-GFDL-GFDL\_ESM2M\_r1i1p1\_SMHI\_RCA4\_v1 -> **GFDL-ESM2M\_RCA4**  
 EUR-44-MPI-M-MPI-ESM-LR\_r1i1p1\_CLMcom-CCLM4-8-17\_v1 -> **MPI-ESM-LR\_CCLM4**

Data are stored on and can be downloaded from DMI’s server (<http://ensemblesrt3.dmi.dk/data/IMPRESSIONS/>) as well as on the IMPRESSIONS data portal

<sup>1</sup> CORDEX is the Coordinated Regional Climate Downscaling Experiment, run by the World Climate Research Program. It aims to advance and coordinate the downscaling of global climate models to regional or local scales.

([www.impressions-project.eu](http://www.impressions-project.eu)). Any queries about the data should be directed to Marianne Sloth Madsen ([msm@dmi.dk](mailto:msm@dmi.dk)) or Cathrine Fox Maule ([cam@dmi.dk](mailto:cam@dmi.dk)).

## Summary

This deliverable documents the climate scenarios that have been prepared for use in IMPRESSIONS. The selected sub-set of GCM-RCM pairs has subsequently been bias-adjusted using quantile mapping for further use by the IMPRESSIONS impact analysts. The European and local case studies mainly rely on bias-adjusted RCM data, but bias-adjusted GCM data may be needed for regions where RCM data are not available. Here, we describe the bias-adjustment method in detail and illustrate how the final climate model data that have been provided are affected by the bias-adjustment.

We describe the WATCH WFDEI data that have been used as the IMPRESSIONS baseline (1981-2010) and compare with the CRU data previously used for the CLIMSAVE baseline (1961-1990). The IMPRESSIONS baseline is warmer by about 1 degree and is generally a bit wetter.

The climate change projections are illustrated in some detail in order to address model spread and hence to represent uncertainties in the projections; 30-year seasonal mean changes (2071-2100 vs. 1981-2010) of temperature, precipitation, short-wave radiation, wind speed, and humidity (both specific and relative) are all shown for each selected GCM-RCM combination to illustrate model spread within the IMPRESSIONS model sub-set. Similar figures are provided for each of the selected GCMs, and we show that the climate change signal of temperature and precipitation to some extent is affected by the dynamical downscaling (by the RCM) as well as by the adopted bias-adjustment procedure.

We also briefly present the climate indices (e.g. number of frost days and consecutive dry days) and climate analogues that have been calculated for Europe to illustrate the projected climate change. Some of these specific indices have been used in the IMPRESSIONS stakeholder workshops per case study to assist with explanations of the regional or local consequences of specific climate developments.

## 1. Introduction

As climate models are not perfect, model simulations for the historical period often show systematic deviations (biases) when compared with observations. This needs to be considered carefully when climate model data are used for impact assessments as the predicted impacts depend on the statistical properties of the climate input. In this Deliverable we describe how the data from the selected climate models were bias-adjusted to provide scenario data suitable for the impact assessments. As IMPRESSIONS includes a large number of impact models and spans local and regional as well as global scales, there is a large variety in the needs for scenario data. Table 2 summarizes the climate scenario data that have been provided within IMPRESSIONS.

The scenarios are all based on the selected core set of climate models but were prepared using different bias-adjustment methods, different baseline periods and reference data sets as well as different temporal and horizontal resolution. The data for the CLIMSAVE Integrated Assessment Platform (IAP2) for Europe and Scotland needed to be consistent with assumptions made in a previous EU project, CLIMSAVE, and, hence, use the Delta Change approach for bias-adjustment and the CRU 1961-1990 baseline data. For consistency within IMPRESSIONS, all scenarios except IAP2 use the WATCH WFDEI data for 1981-2010 to represent the baseline, and GCM as well as RCM data are bias-

adjusted using the same quantile-quantile bias-adjustment method. Note that the IAP2 is being replaced by the rIAM model within IMPRESSIONS, so all scenarios in the latter stages of the project will be based on a consistent approach.

**Table 2: Overview of the climate data sets provided in IMPRESSIONS.**

	Region	Baseline	Horizontal resolution	Time resolution	Methodology
IAP2 - Europe	Europe	CRU 1961-1990	10'	30-year time slices	Delta change
IAP2 - Scotland	Scotland	UKCP09 1961-1990	5km	30-year time slices	Delta change
WATCH WFDEI Baseline data	Global	WFDEI 1981-2010	0.5°	Daily data	Original data
WATCH WFDEI Baseline data	Europe	WFDEI 1981-2010	10'	Daily data	Regridding and lapse-rate correction <sup>2</sup>
Bias-adjusted RCM data	Europe (EU)	WFDEI 1981-2010	0.5°	Daily data	Bias-adjustment, Quantile mapping
Bias-adjusted RCM data	Europe (EU10)	WFDEI 1981-2010	10'	Daily data	Regridding and lapse-rate correction
rIAM	Europe	WFDEI 1981-2010	10'	Decadal time slices	Averaging and reformatting of bias-adjusted data (EU10)
Bias-adjusted GCM data	-60-60°E, 0-90°N	WFDEI 1981-2010	0.5°	Daily data	Bias-adjustment, Quantile mapping

In Section 2 we describe the bias-adjustment methods and the WATCH WFDEI reference data used for the 1981-2010 baseline period. In Section 3, the bias-adjusted RCM and GCM data are presented and Section 3.3 provides a comparison of the GCM vs. RCM climate change signal before and after the bias-adjustment. In Section 4, we illustrate the behavior of a number of selected climate indices. In the last section we briefly describe the progress in developing probabilistic scenarios.

## 2. Bias-adjustment of climate scenario data

Climate data from RCMs and GCMs generally suffer from biases in more or less all variables. The biases differ from model to model, variable to variable and with season; examples of the biases of one of the RCMs used in IMPRESSIONS are shown in Figure 2.1. Many models are able to reproduce temperatures within a few degrees, but biases of several tens of percent are not uncommon (e.g. precipitation over Europe). Biases of this level are often problematic when the climate model output is to be used as input in impact models such as hydrological models. Therefore a bias-adjustment is applied to the

<sup>2</sup> This is described in Section 2.2.

---

climate model output to make it have the same statistical properties as observations during a specified calibration period. In IMPRESSIONS, this calibration period is taken to be 1981-2010.

The most simple bias correction methods are ‘Delta Change’ methods in which the mean observed value is adjusted by applying a correction for the future that is derived from climate models. This method was used in the CLIMSAVE project and so was reproduced for the CLIMSAVE IAP2 model data for Europe and Scotland in IMPRESSIONS. As the IAP2 data include 30-year monthly mean data, the Delta Change method is a reasonable approach.

However, as some of the impact models involved in IMPRESSIONS rely on climate data with daily resolution we have chosen to use quantile mapping for the main bias-adjustment; this method has been proven to perform well compared to other bias-adjustment methods (Räty et al., 2014). Bias-adjustment requires an observational data set to bias adjust against and to this end we use the WATCH WFDEI which is a global data set based on re-analysis and with sub-daily resolution (Weedon et al 2011, 2014). In Section 2.1 we describe the bias-adjustment methods and in Section 2.2 we describe the WATCH WFDEI climatology for 1981-2010 and compare it with the more well-known CRU 1961-1990 climatology used in CLIMSAVE.

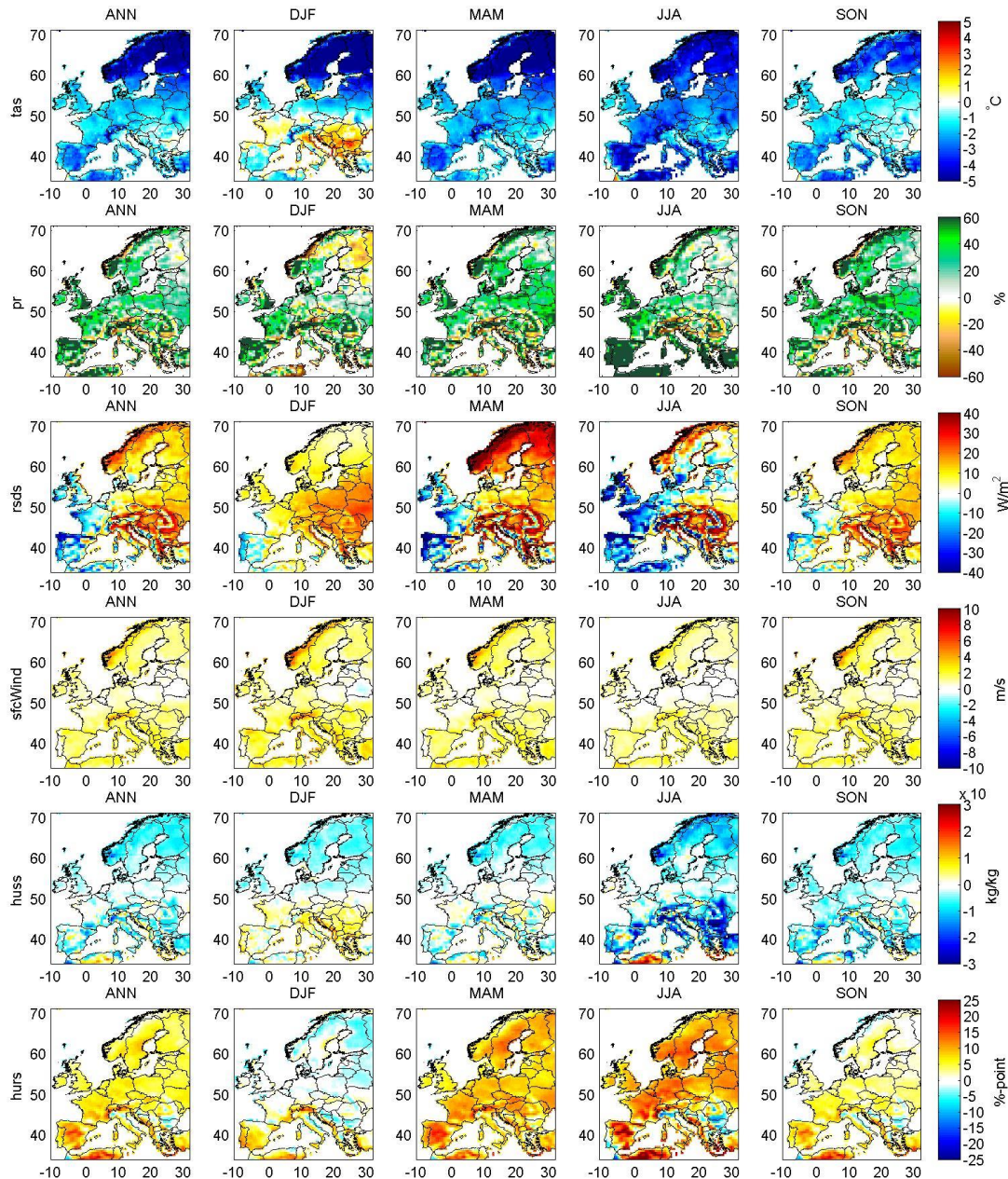


**Figure 2.1: Bias of GFDL-RCA compared to WFDEI prior to bias correction for temperature (tas), precipitation (pr), short wave radiation (rsds), surface wind (sfcWind), specific humidity (huss) and relative humidity (hurs). Both annual (ANN) and seasonal (DJF, MAM, JJA, SON) means are shown, all values are averages over 1981-2010.**

## 2.1. Bias-adjustment methods

The bias-adjustment methods used in IMPRESSIONS are described below; the Delta Change method is briefly described in Section 2.1.1 and the quantile mapping procedure is explained in more detail in Section 2.1.2.

### 2.1.1. Delta Change

The first set of IMPRESSIONS scenario data (IAP2 for Europe and Scotland) were prepared using the same methods and baseline data as in the CLIMSAVE project. However, the GCM-RCMs selected for IMPRESSIONS were used and the scenarios were extended until 2100.

In the Delta Change approach, the observed data is used as the baseline which is combined with the simulated mean change deduced from the climate model simulations to produce future climate scenarios. For temperature, the absolute change in temperature is added to the observed baseline temperature and for precipitation and solar radiation the relative changes are applied by multiplication.

For the European IAP2, the changes in climate variables were calculated on the RCM grid (~50km) and remapped to the CRU 10'x10' grid using bilinear interpolation for temperature and a conservative method (Jones 1999) for precipitation and radiation.

The Scottish version of the IAP2 uses the 5x5 km UKCP09 climatology 1961-1990 as the baseline. It includes the same variables as the European IAP2 but also the wind speed for which the relative change is applied by multiplication. All changes were calculated on the RCM grid (~50 km) and remapped to the 5x5 km resolution using distance weighted averaging.

An advantage of the Delta Change method is that it is relatively quick to add new scenario data; for instance a set of RCP2.6 data were added to the core set of scenario data to explore impacts under 1.5°C scenarios. These RCP2.6 scenario data are only available for IAP2.

Note that, even though the rIAM scenario data are similar to the IAP2 data in many respects, the rIAM data are not prepared using the Delta Change method. Instead the rIAM data were prepared as decadal averages of the daily data bias-adjusted using the quantile mapping described below. This was to assure consistency between the scenarios used within the project.

### 2.1.2. Quantile mapping

In IMPRESSIONS, daily RCM output for the core set of scenarios has been bias-adjusted using an empirical statistical quantile-quantile mapping. This method has been shown to perform well in comparison with other bias-adjustment methods and Delta Change methods (Räty et al., 2014).

Time series of daily data from the RCMs are bias corrected against daily time series of observations from the WFDEI data set. The calibration period used is 1981-2010; as the historical simulations of the RCMs end with 2005, the period 2006-2010 are taken from the simulations following the RCP4.5 scenario.

The bias-adjustment method used is an empirical statistical quantile mapping (Thiemeßl et al, 2012, Wilcke et al., 2013). Each variable is bias corrected independently; studies have shown that the inter-variable dependencies of the variables are retained by the quantile mapping (Wilcke et al., 2013). The bias-adjustment is done against gridded observation data, so the first step is to regrid the RCM output onto the grid of the observations. Mean, maximum and minimum temperatures are regridded using bilinear interpolation, and a lapse rate correction of 0.006K/km is applied to account for elevation differences. Precipitation, specific humidity and shortwave radiation are regridded using a conservative interpolation. The bias-adjustment is done grid cell by grid cell and thereby accounts for geographical variation.

The central feature in quantile mapping is the cumulative distribution function (ECDF), which is constructed by using data from a given calibration period. To produce a bias corrected data set, which has the same statistical properties as the observed data, the ECDF constructed from the RCM output is fitted to the ECDF of the observations. If a simulated RCM value of e.g. temperature is exceeded with a certain probability in a reference simulation, it will be translated to the corresponding observational value with the same exceedance probability in the observational data set (see Figure 2.2). To take seasonal variation into account, the ECDFs are built for each day of the year (doy) using a 31-day sliding window, i.e. the ECDF of the 16<sup>th</sup> of January is made from all the values of January 1<sup>st</sup> to January 31<sup>st</sup> from the entire calibration period. As the calibration period is 30 years, 930 values are used in this case for constructing each ECDF. For this study we have chosen to build the ECDFs empirically (i.e. directly from the data without smoothing or fitting a function) by simply binning the modelled and observed variables, thereby no assumptions on the underlying distribution of the variables needs to be made. The bin size used depends on the variable; we have used a bin size of 0.1 K for temperatures, and 0.1 mm/day for precipitation.

Figure 2.2 shows a graphical example of the bias-adjustment process, using mean temperature, of the ECDFs of the observations and an RCM simulation in a given grid point. Once the ECDFs have been built for both the observed and the modelled parameter, the next step is to look at the probabilities of the individual RCM values. So looking at the given temperature,  $x^{rcm,raw}$ , at time  $t$ , corresponding to a given day of year (*doy*), in grid point  $i$  the probability,  $p_{t,i}$ , is determined for that temperature from the ECDF of the RCM output from the calibration period (*cal*):

$$p_{t,i} = ECDF_{doy,i}^{rcm,cal}(x_{t,i}^{rcm,raw})$$

The next step is to calculate a correction term,  $\Delta x_{t,i}$ , by taking the difference between the inverse ECDF of the observations and the raw RCM output from the calibration period for the given *doy* for that probability:

$$\Delta x_{t,i} = ECDF_{doy,i}^{obs,cal^{-1}}(p_{t,i}) - ECDF_{doy,i}^{rcm,cal^{-1}}(p_{t,i})$$

The correction term is then added to the raw RCM temperature,  $x^{rcm,raw}$ , to give the bias corrected temperature,  $x^{rcm,cor}$ :

$$x_{t,i}^{rcm,cor} = x_{t,i}^{rcm,raw} + \Delta x_{t,i}$$

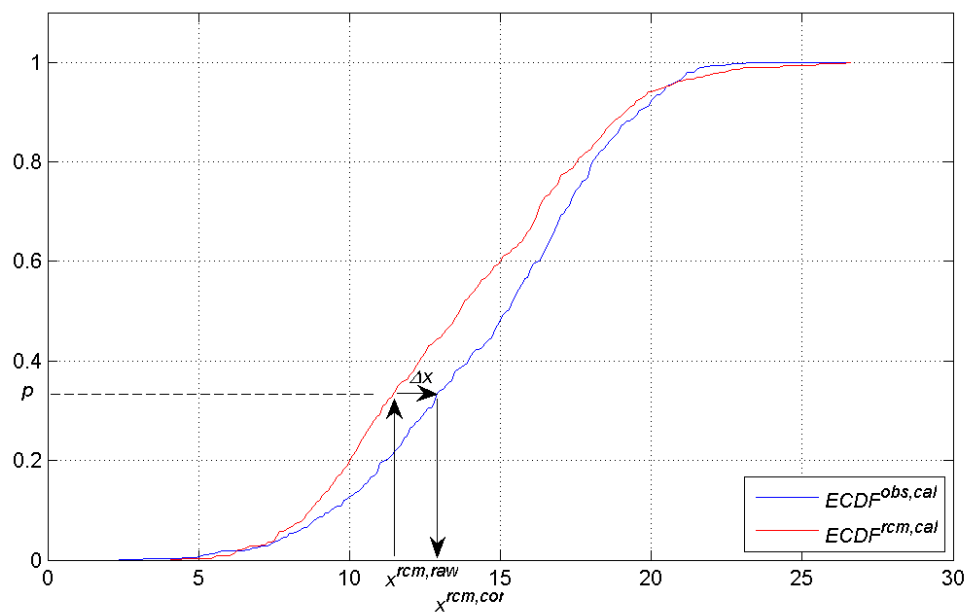


**Figure 2.2:** Graphical interpretation of the bias-adjustment for mean temperature. For a specific value of the minimum temperature from the RCM of the same day of the year (doy),  $x^{rcm,raw}$ , the probability,  $p$ , is determined from the ECDF of the RCM of the calibration period,  $ECDF^{rcm,cal}$ . This probability is then translated to the corrected temperature,  $x^{rcm,cor}$ , from the ECDF of the observations in the calibration period,  $ECDF^{obs,cal}$ .

The RCM values of the future time slices may be higher than the highest RCM values of the calibration period. In these cases the correction applied is the correction of the highest RCM values of the calibration period. Similarly if an RCM value of the future time-slices is lower than the lowest RCM value of the calibration period, the correction term of the lowest RCM value of the calibration period is applied.

The bias-adjustment procedure described above is used for mean temperature and the main part of it is the same for all the variables, but several of the variables have some special features:

- **Radiation:** The bias-adjustment procedure may create negative values of the radiation, which is physically impossible. Such values have been corrected to zero. For grid points where the incoming short-wave radiation at the surface is zero for a given day of the year throughout the calibration period of both the model and the observations, all future values are set to zero as well (this occurs for winter months at high northern latitudes).
- **Minimum and maximum temperature:** Using the empirical statistical bias-adjustment method on minimum, maximum and mean temperature separately can lead to cases where minimum temperature may exceed mean or even maximum temperature, which is inconsistent. To avoid these inconsistencies we have calculated the daily temperature range (dtr) from maximum and minimum temperature for both the models and the observations, and bias-adjusted this, as well as the ratio between maximum and mean temperature. From the bias-adjusted daily temperature range, mean temperature and the ratio between maximum and mean temperature, we have derived bias-adjusted minimum and maximum temperatures.
- **Precipitation:** For precipitation a frequency adaptation (Themeßl et al., 2012) is applied to prevent dry days being mapped into wet days in cases where the dry day frequency in the raw RCM output

is higher than the observed number of dry days. We use a threshold of 1 mm/day, and for wet days ( $\geq 1$ mm/day) a bin size of 0.1 mm/day is used, whereas we use a bin size of 0.01 mm/day for dry days ( $< 1$ mm/day). The essence of the frequency adaptation is to generate dry days in the first bin (i.e. 0 – 0.01 mm/day) of the RCM output by randomly sampling the observations of the same bin. By doing this the number of dry days is conserved. However, the most common situation is that the RCMs have too many days with light precipitation (drizzling-effect) and the quantile mapping efficiently corrects this known bias.

- **Humidity:** For the WFDEI observational data, as well as for several of the GCMs and RCMs used in IMPRESSIONS only specific humidity (not relative humidity) is available. Therefore the bias-adjustment is done on the specific humidity, and the relative humidity is estimated from the bias-adjusted specific humidity, the pressure, and the bias-adjusted mean temperature using the Arden Buck equation.

## 2.2. The WATCH WFDEI baseline data

The WATCH WFDEI daily data ( $0.5^\circ$ ) is used as the baseline data in IMPRESSIONS. This data set was selected as it has global coverage and at the same time includes sub-daily data of a large number of climate variables needed for the hydrological modelling. Seasonal means (1981-2010) of air temperature (tas), precipitation (pr), shortwave downward radiation (rsds), 10 m wind speed (sfcWind), specific (huss) and relative (hurs) humidity are shown in Figure 2.3. Note, that relative humidity is not a WATCH WFDEI variable but is estimated from the specific humidity, pressure and temperature using the Arden Buck equation.

The WATCH data is based on ERA-Interim reanalysis but monthly averages have been bias-adjusted against the CRU observational data. The temperature data were bias-adjusted against CRU mean monthly temperature and diurnal temperature range; precipitation was bias-adjusted against observations by first correcting the number of dry days and then scaling the precipitation in each time step to make the monthly means match the observations. As the last step, an under-catch correction has been applied (for snow and rain separately) to account for the anticipated underestimation of precipitation in the observed data (Adam and Lettenmaier, 2003). Two separate sets of precipitation data exist, one that is bias corrected against CRU TS3.1/TS3.101/TS3.21 and one that is bias corrected against GPCC v5/v6 (Schneider et al., 2011). We have followed the general recommendation and used the GPCC corrected data set in IMPRESSIONS as this data set is based on data from more stations. More information on the WATCH methodology can be found in Weedon et al (2011, 2014) and references therein. Please note that Weedon et al (2014) should be cited in publications using WATCH WFDEI data.

As high-resolution ( $10'$ ) data were requested by the European case study, the original  $0.5^\circ$  WATCH WFDEI data were remapped to the  $10'$  grid. Temperature and wind were remapped by bilinear interpolation and temperature data were height-corrected using a lapse rate correction of 0.006K/m. Precipitation, radiation and humidity data were remapped using a conservative method (Jones 1999).

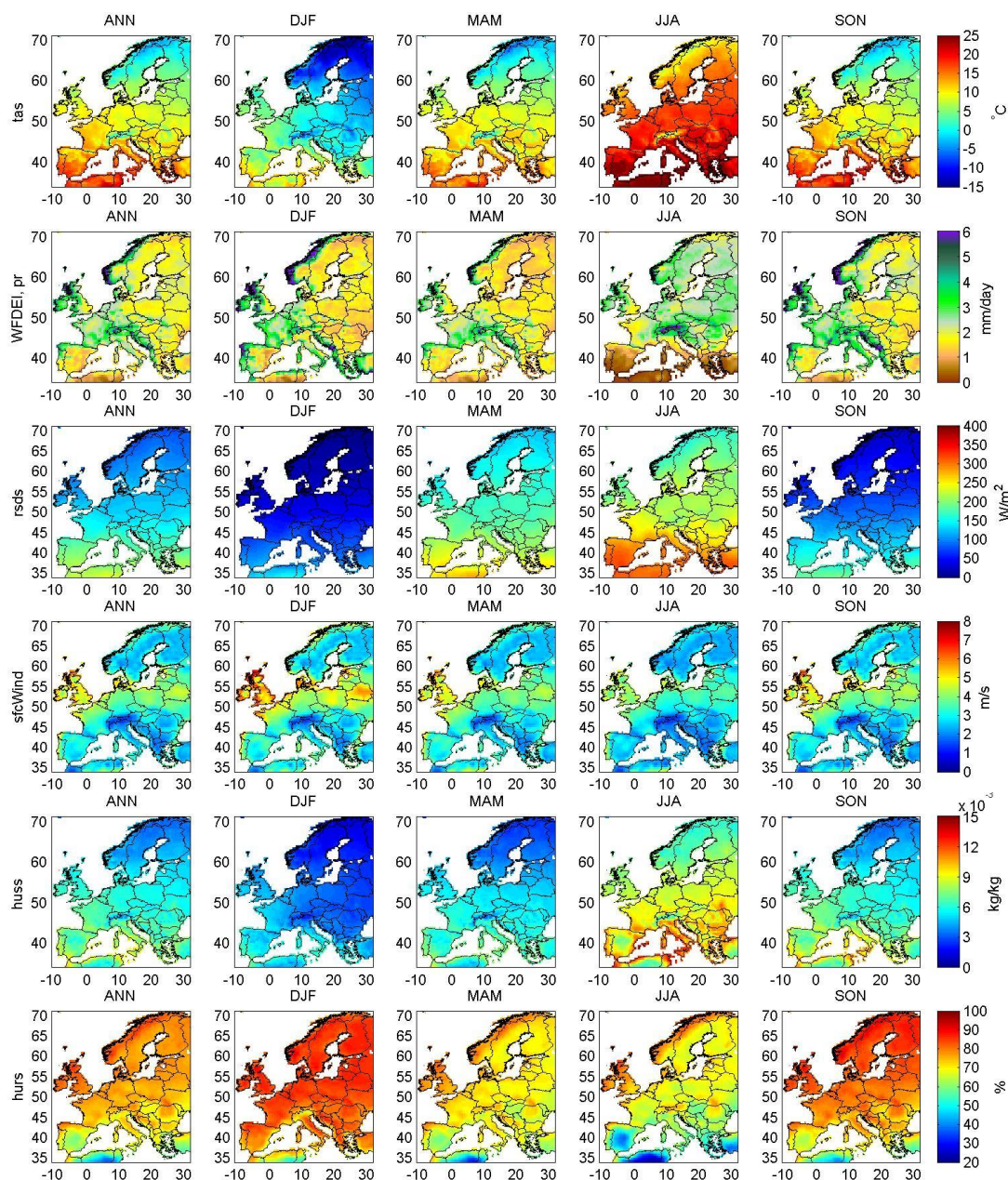


**Figure 2.3: Annual (ANN) and seasonal (DJF, MAM, JJA, SON) means of temperature (tas), precipitation (pr), radiation (rsds), wind (sfcWind), specific (huss) and relative humidity (hurs) from the Watch WFDEI data set from 1981-2010. Note that relative humidity has been derived from specific humidity using the Arden Buck Equation as described in the text.**

In CLIMSAVE, the CRU 1961-1990 climatology ( $10'$ ) was used as the baseline. As the WATCH WFDEI was not well-known to the impact modellers, we did a small comparison to explore the differences between the two baseline periods and more generally between the CRU and WATCH data sets. The comparison was performed for temperature and precipitation and was documented in an IMPRESSIONS technical note<sup>3</sup>. Figures 2.4 and 2.5 show the differences between the climatology of

<sup>3</sup> [http://ensemblest3.dmi.dk/data/IMPRESSIONS/WFDEI/IMPRESSIONS\\_baseline\\_comparison.pdf](http://ensemblest3.dmi.dk/data/IMPRESSIONS/WFDEI/IMPRESSIONS_baseline_comparison.pdf)

mean temperature and precipitation for WATCH WFDEI 1981-2010 vs. CRU 1961-1990 after downscaling to the CRU 10' grid.

Overall, we found that the WATCH and CRU monthly mean temperature data compare very well at the 0.5° resolution as expected since the WATCH data was bias-corrected against CRU monthly mean temperature. The temperature difference of about 1°C warming between WATCH WFDEI 1981-2010 and CRU 1961-1990 reflects a general warming between the two time periods. Differences between CRU and WATCH are however found in minimum and maximum temperature, because the diurnal temperature range was used for the bias correction of WATCH WFDEI and the relationship with mean temperature is defined differently in the two data sets. A comparison between the high-resolution data (CRU vs. WATCH) revealed some inconsistencies in the CRU data which are described in more detail in the IMPRESSIONS technical note.

For precipitation, the differences between the two climatologies are larger. The differences reflect that the WATCH WFDEI data were bias-adjusted against the GPCC precipitation data (and not CRU), and furthermore, the applied under-catch correction increases the amount of precipitation especially in regions where snowfall is the dominant form of precipitation.

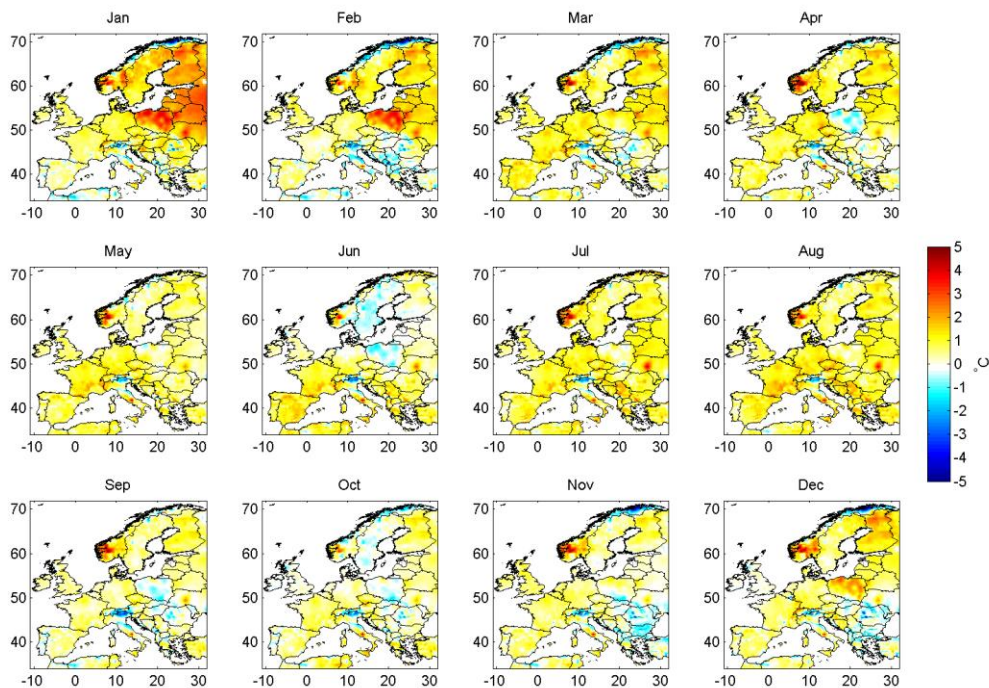


**Figure 2.4: Monthly mean difference in mean temperature (°C) for WATCH WFDEI 1981-2010 vs CRU 1961-1990 (10').**

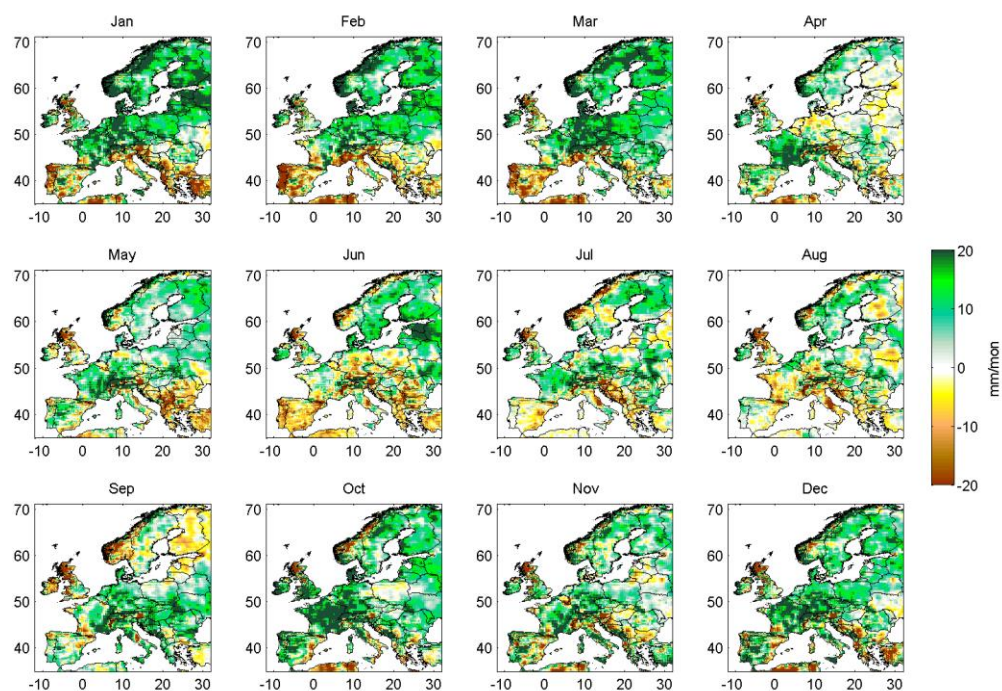


**Figure 2.5: Monthly mean difference in precipitation (mm/month) for WATCH WFDEI 1981-2010 vs. CRU 1961-1990 (10').**

### 3. Climate change projections

In this section the bias-adjusted climate change projections are considered. First we illustrate the changes in mean climate change projected by the core set of RCMs. Similar results are presented next for the bias-adjusted GCMs and, finally, we compare the climate change signal projected by GCM vs RCM, and bias-adjusted data vs model outputs.

#### 3.1. Bias-adjusted RCM data

In this section we describe the climate change projections based on the bias-adjusted RCMs. First we consider one single model, and consider the 30-year mean seasonal climate change signal simulated for each variable for each of the periods 2011-2040, 2041-2070 and 2071-2100. Next we compare the spread in the climate change signal for the last period (2071-2100) across all seven RCMs.

Figure 3.1 illustrates the CORDEX domain in which the RCM data are available and the sub-domain for which the RCM data have been bias-adjusted. The bias-adjustment was performed at the resolution of the WATCH reference data (0.5°) which is quite similar to the resolution of the RCM data. As higher resolution data were requested for the European case study, the data were interpolated to the 10' CRU grid after bias-adjustment. As for the WATCH data, temperature and wind speed data were bilinearly interpolated and a lapse rate correction was applied for temperature. Precipitation, radiation and humidity were remapped using a conservative method. Decadal monthly averages were extracted for a slightly smaller European domain used by the regional integrated assessment model

(rIAM). It should be stressed that the high resolution data are based on interpolations and do not include additional information.

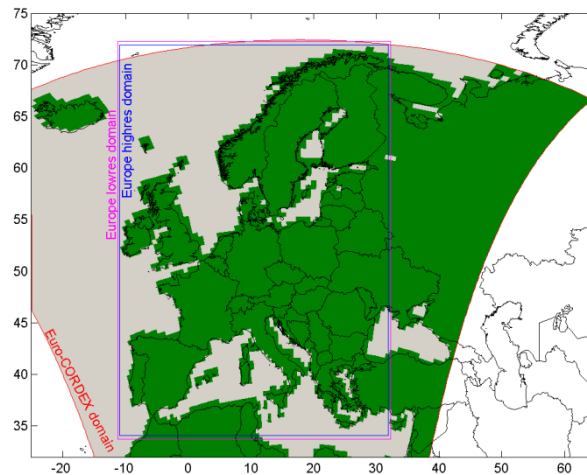


**Figure 3.1: Map showing the CORDEX domain for which the RCM data is available, and the blue and pink boxes show the areas in which bias-adjustment has been done; the pink box illustrates the 0.5° grid and the blue box the 10' grid.**

The bias-adjustment significantly reduces bias on each variable. This is illustrated in Figure 3.2 which shows the biases of the bias-adjusted values of GFDL-RCA4 and may be directly compared to Figure 2.1, which shows the bias prior to bias-adjustment. Note that the scales of the individual axes are different in this figure; otherwise all the maps would be completely represented in white.

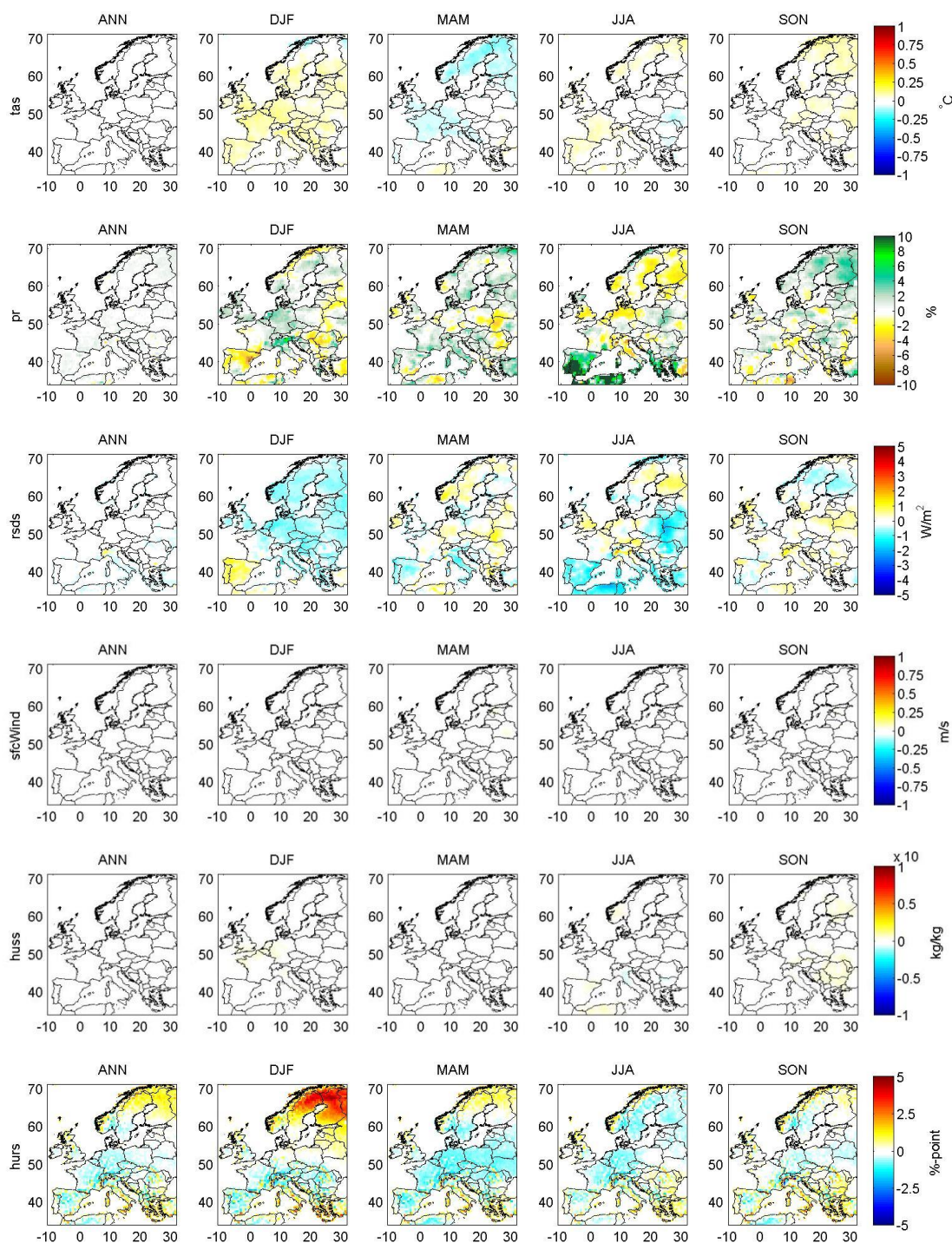


**Figure 3.2: Bias of the bias-adjusted annual (ANN) and seasonal (DJF, MAM, JJA, SON) means of GFDL-RCA 1981-2010 of temperature (tas), precipitation (pr), short wave radiation (rsds), surface wind (sfcWind), specific humidity (huss) and relative humidity (hurs). Note the different scales on the axes compared to Figure 2.1.**

Also note, that for simplicity we have used the WATCH WFDEI data as the baseline data for the rIAM independent of the GCM/RCM used for the scenario period. As the rIAM is using the bias-adjusted climate data for the future time slices, it would be more consistent to use the bias-adjusted baseline data for each of the GCM-RCMs. However, as each of them through the bias-adjustment is given the

same statistical properties as the observations of the baseline period, differences will be very small (*cf.* the bias shown in Figure 3.2).

From the bias-adjusted RCM data, projected changes in all the climate variables can be calculated. Figures 3.3 to 3.10 show climate changes in annual and seasonal means for 2011-2040, 2041-2070 and 2071-2100 compared to 1981-2010 for CanESM-CanRCM (RCP8.5) for mean temperature (Figure 3.3), precipitation (Figure 3.4), short-wave radiation (Figure 3.5), wind speed (Figure 3.6), specific humidity (Figure 3.7), relative humidity (Figure 3.8), maximum temperature (Figure 3.9) and minimum temperature (3.10).

For the CanESM-CanRCM model, the temperature shows a rather uniform pattern of change that increases towards the end of the century. In winter, the largest change is found in northern Europe; in summer the largest temperature increases are found in southern Europe (Figure 3.3). For precipitation, we also see an increased climate change towards the end of the century; the general pattern is increased precipitation to the north and a decrease to the south (Figure 3.4). The changes in incoming short-wave radiation are much more diverse. The model shows a large increase in central Europe during summer and also a general increase in autumn, except for northern Scandinavia (Figure 3.5). Changes in wind are not very uniform and the most pronounced changes seem to be a decrease in mean wind speed during summer and an increase during winter especially in Scandinavia and Central Europe (Figure 3.6). This pattern also intensifies towards the end of the century. Figure 3.7 shows that the specific humidity increases with a pattern very similar to the pattern of temperature change. The relative humidity also generally increases but in regions with high increase in temperature combined with a decrease in precipitation, a decrease in relative humidity is projected during summer and autumn (Figure 3.8).

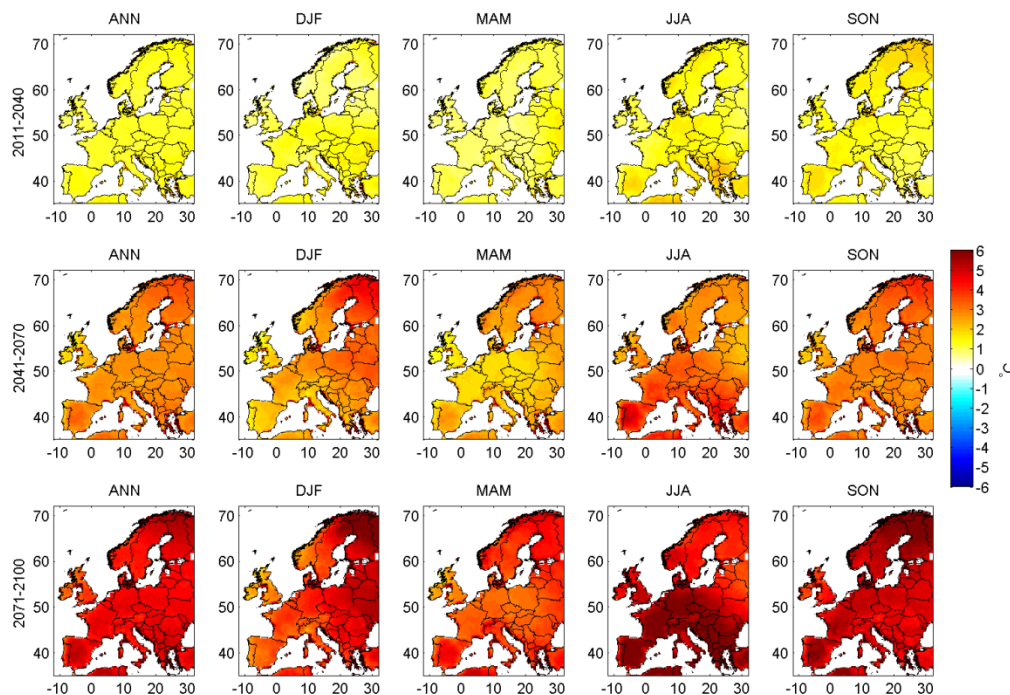


**Figure 3.3: Projected annual (ANN) and seasonal (DJF, MAM, JJA, SON) changes in temperature (°C) for three time periods from CanESM-CanRCM RCP8.5 with respect to 1981-2010.**

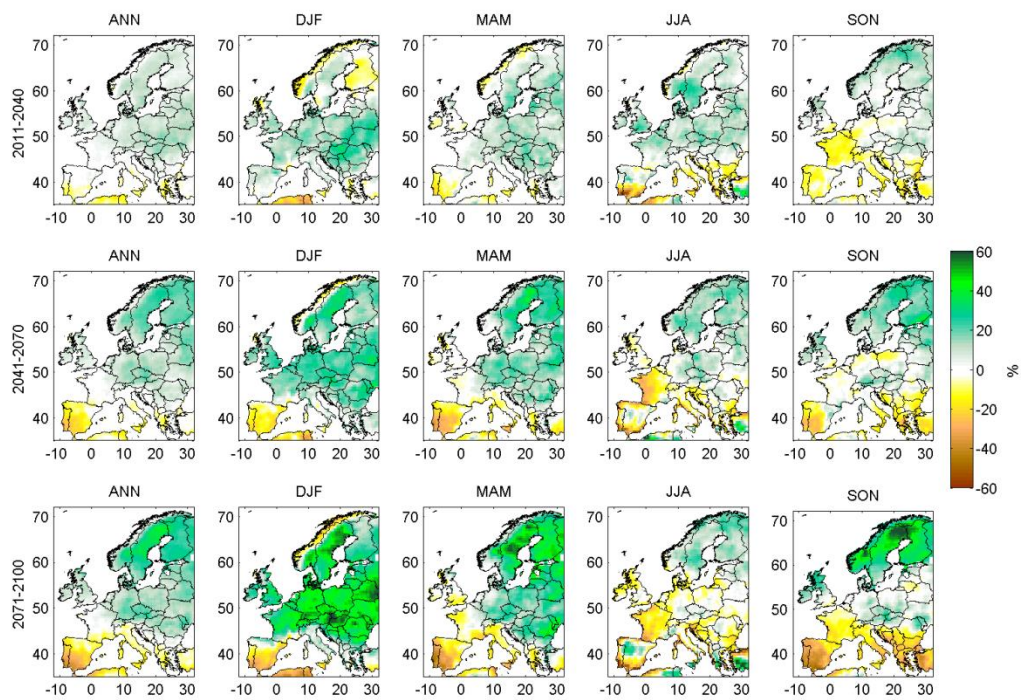


**Figure 3.4: Projected annual (ANN) and seasonal (DJF, MAM, JJA, SON) changes in precipitation (%) for three time periods from CanESM-CanRCM RCP85 with respect to 1981-2010.**

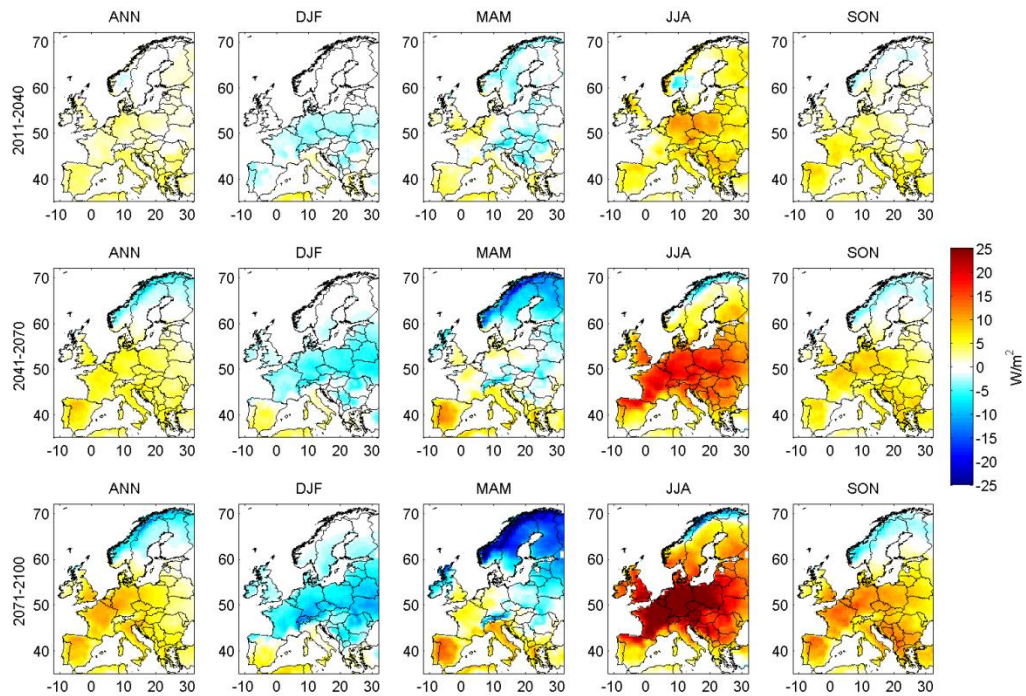


**Figure 3.5: Projected annual (ANN) and seasonal (DJF, MAM, JJA, SON) changes in short-wave radiation ( $Wm^2$ ) for three time periods from CanESM-CanRCM RCP85 with respect to 1981-2010.**

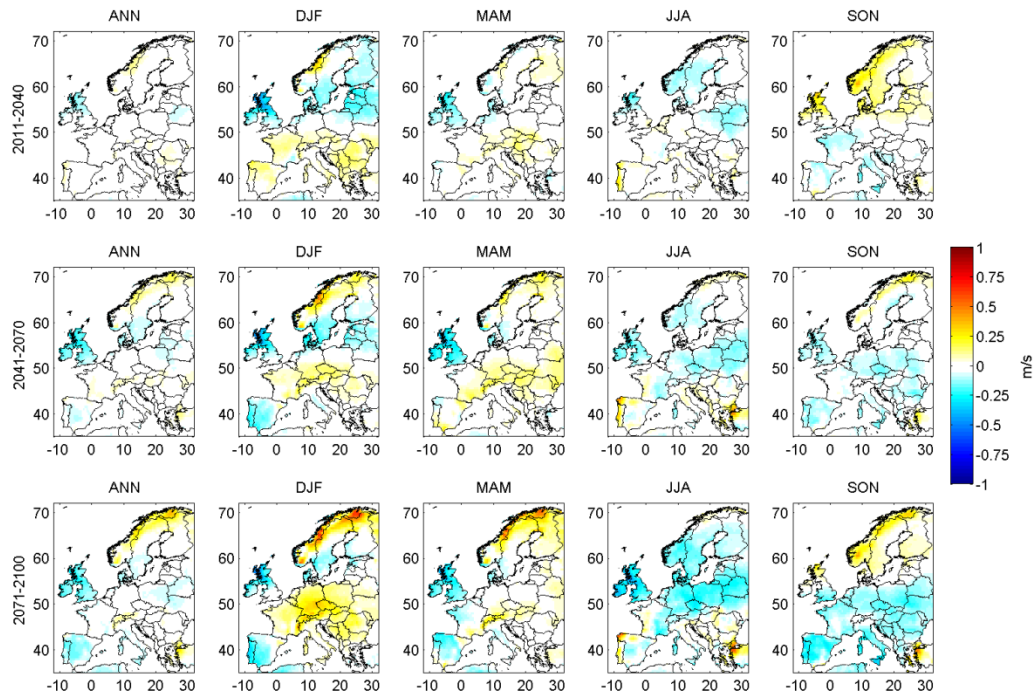


**Figure 3.6: Projected annual (ANN) and seasonal (DJF, MAM, JJA, SON) changes in surface wind speed (at 10 m, m/s) for three time periods from CanESM-CanRCM RCP85 with respect to 1981-2010.**

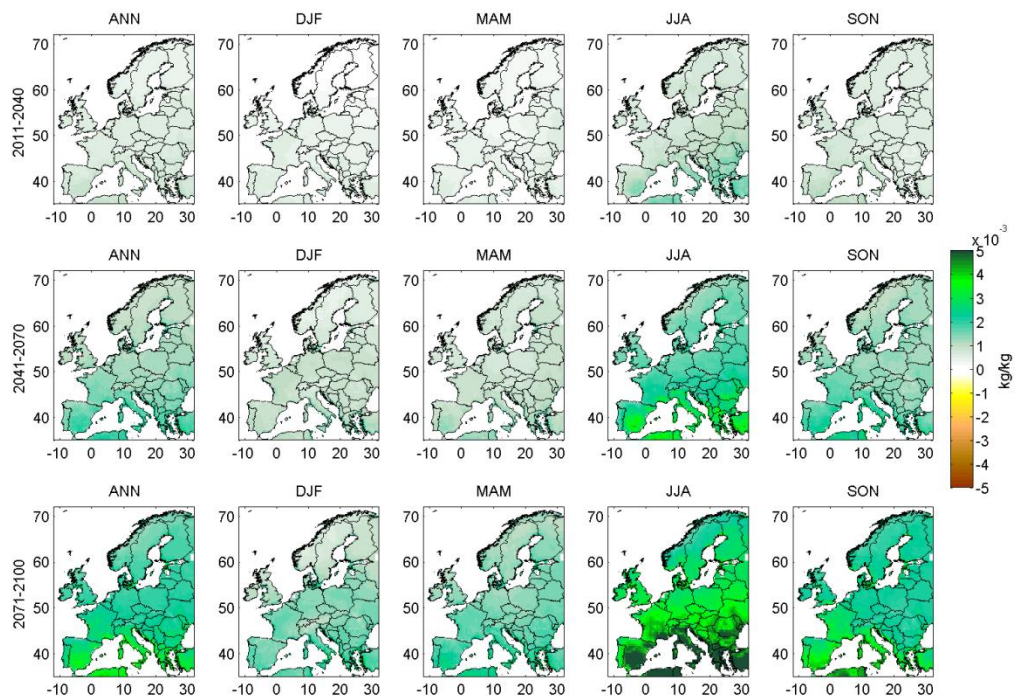


**Figure 3.7: Projected annual (ANN) and seasonal (DJF, MAM, JJA, SON) changes in specific humidity (kg/kg) for three time periods from CanESM-CanRCM RCP85 with respect to 1981-2010.**

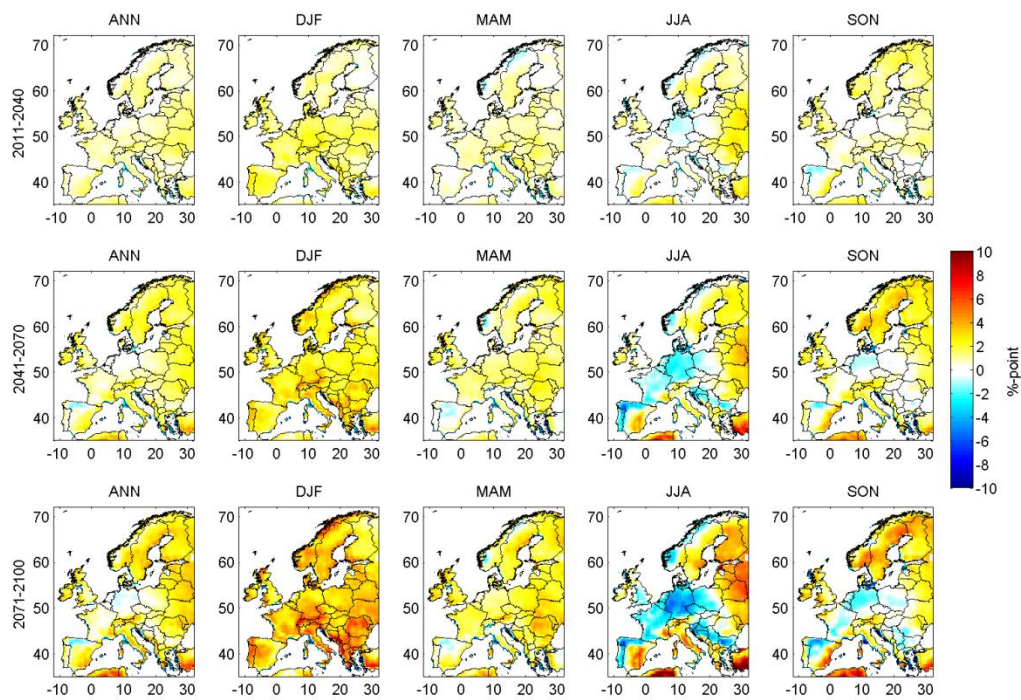


**Figure 3.8: Projected annual (ANN) and seasonal (DJF, MAM, JJA, SON) changes in relative humidity (%-point) for three time periods from CanESM-CanRCM RCP85 with respect to 1981-2010.**

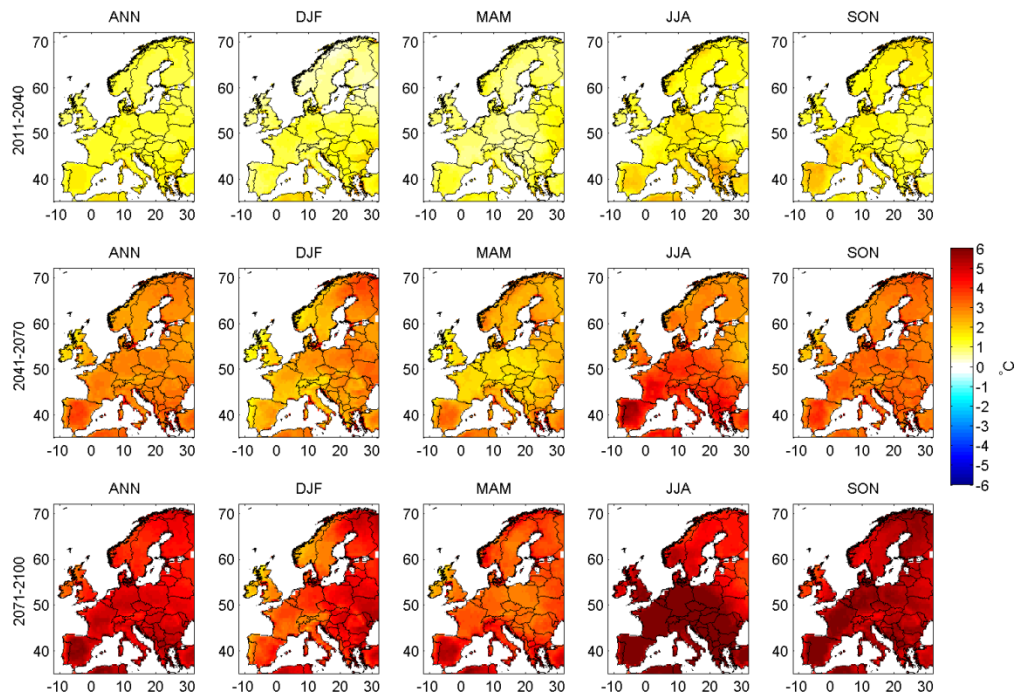


**Figure 3.9: Projected annual (ANN) and seasonal (DJF, MAM, JJA, SON) changes in maximum temperature (°C) for three time periods from CanESM-CanRCM RCP85 with respect to 1981-2010.**

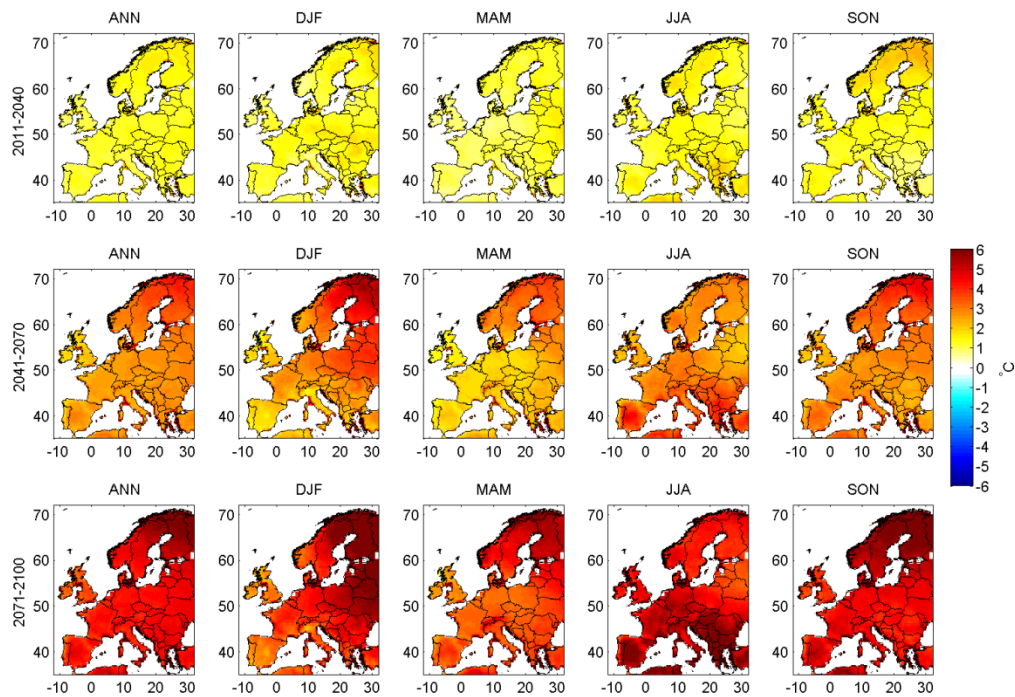


**Figure 3.10: Projected annual (ANN) and seasonal (DJF, MAM, JJA, SON) changes in minimum temperature ( $^{\circ}\text{C}$ ) for three time periods from CanESM-CanRCM RCP85 with respect to 1981-2010.**

Figures 3.11-3.16 show the climate change signal for the last time period (2071-2100 vs. 1981-2010) for each variable and for each of the seven GCM-RCMs in the core set. The temperature signal clearly illustrates the large spread between high-end, intermediate and low-end scenarios (Table 1, Figures 3.11 and 3.24). For precipitation, the models in general agree that precipitation will increase in northern Europe whereas southern Europe will have drier conditions (Figure 3.12). However, the models vary in strength of the signal and also in the seasonal and geographical variation. All selected models agree on an increase in specific humidity (Figure 3.15) and the increase correlates with the models projected temperature increase. The spread in the projected change in relative humidity (Figure 3.16) seems to be related to the spread in changes in temperature as well as precipitation. For wind speed the models do not agree on either the sign of the change or its seasonal variation (Figure 3.14).

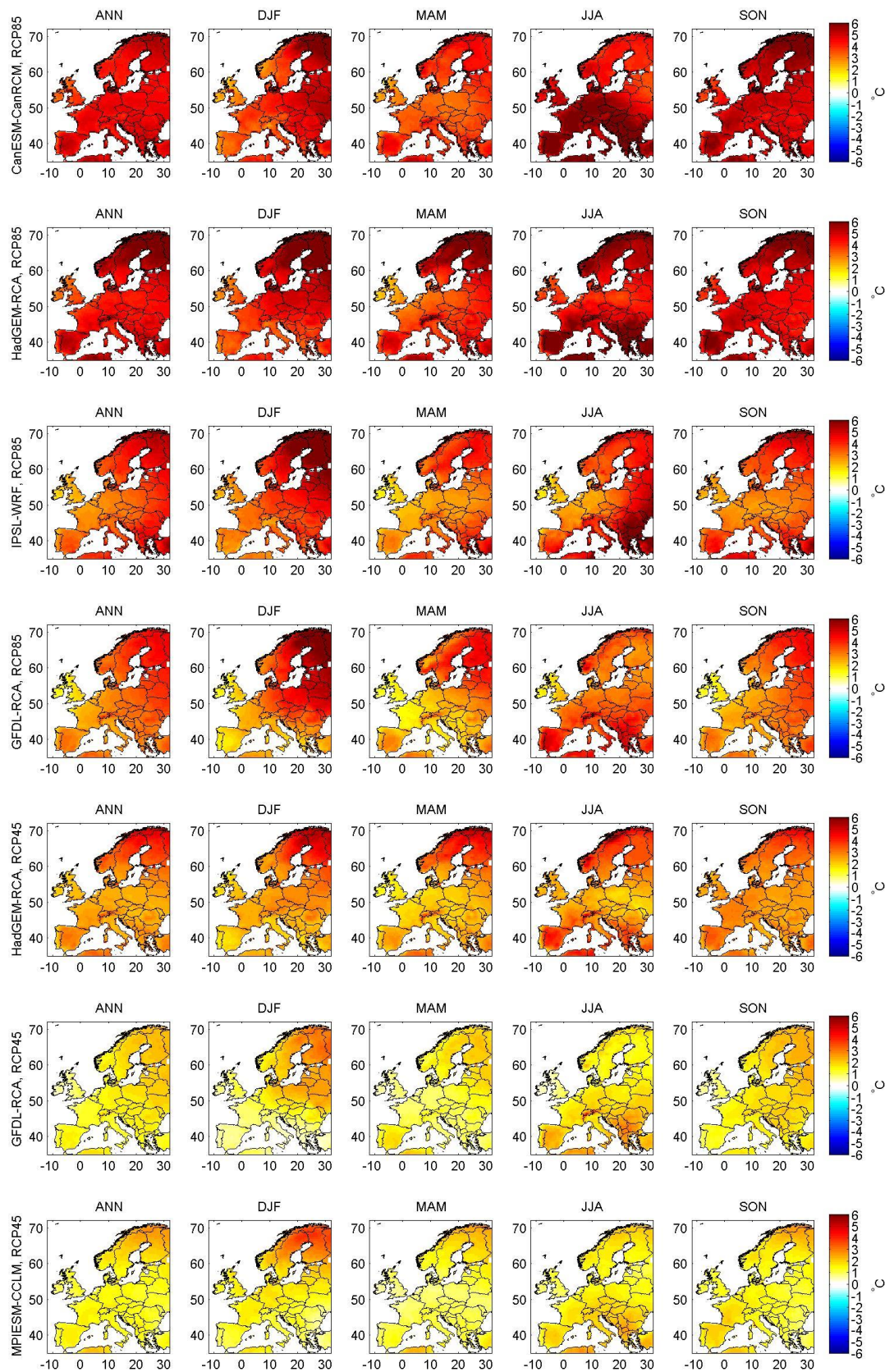
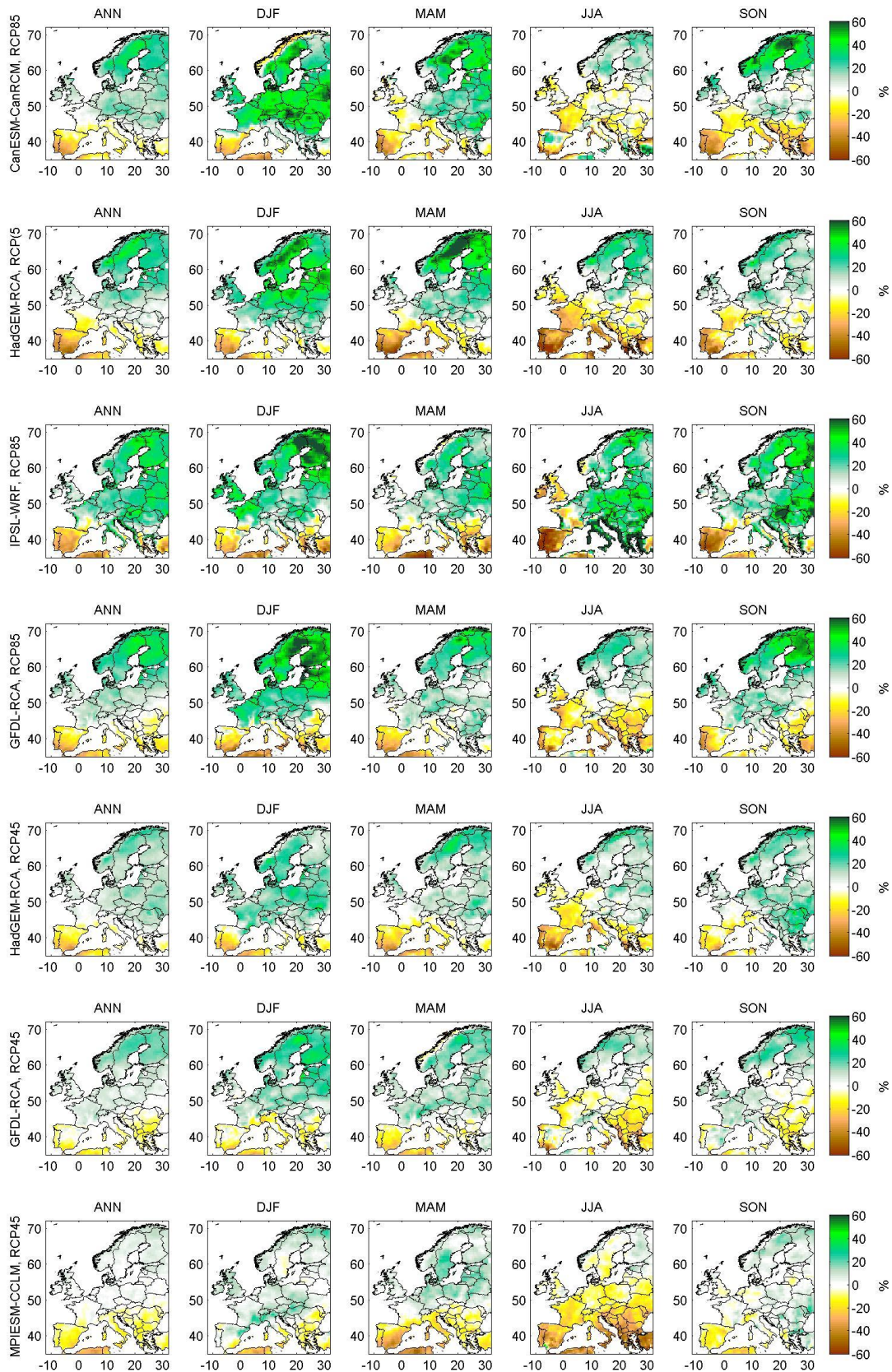


Figure 3.11: The climate change signal of temperature (2071-2100 minus 1981-2010) for all 7 models used in IMPRESSIONS illustrating model spread.



**Figure 3.12: The climate change signal of precipitation (2071-2100 relative to 1981-2010) for all 7 models used in IMPRESSIONS illustrating model spread.**

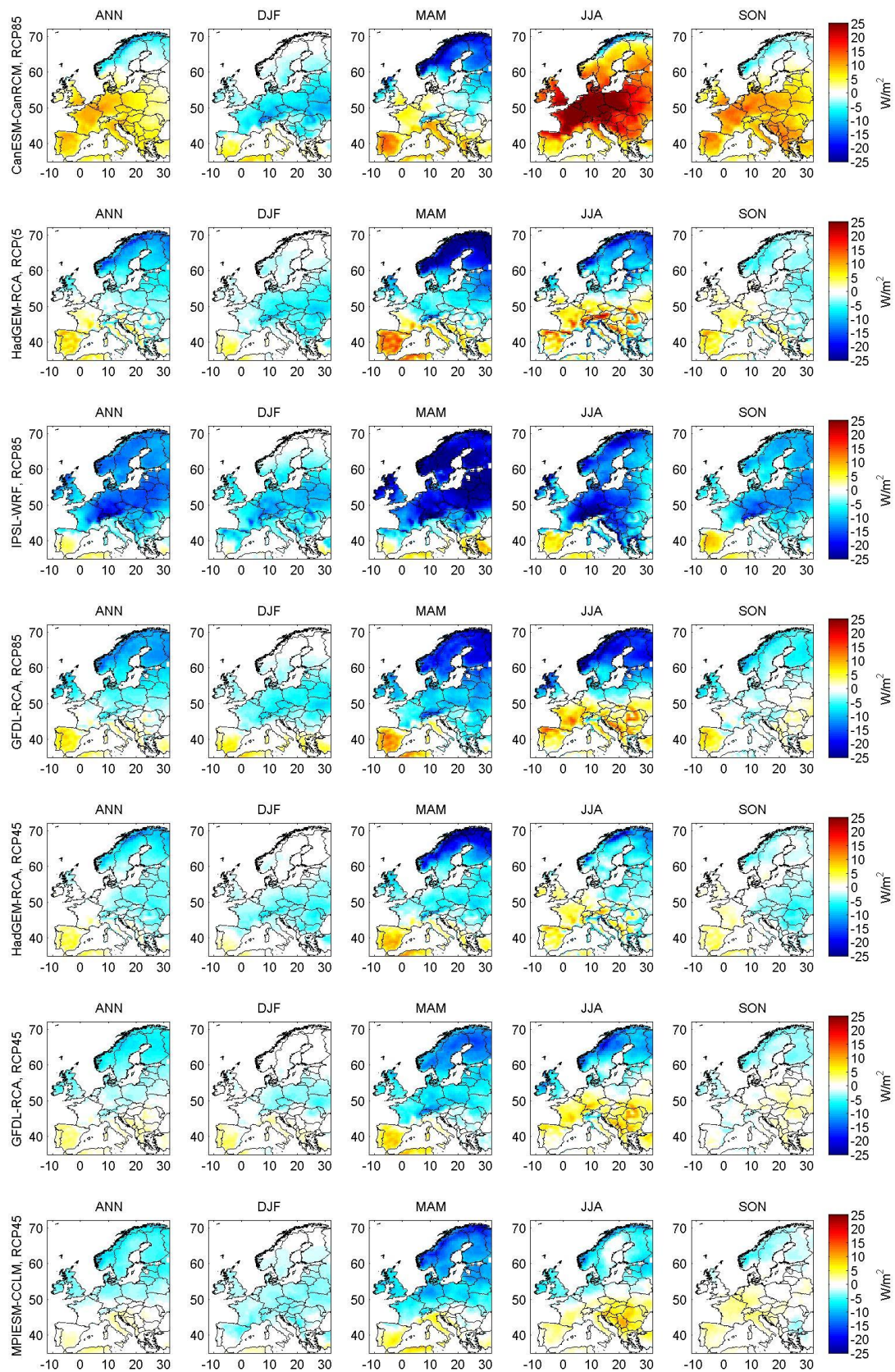
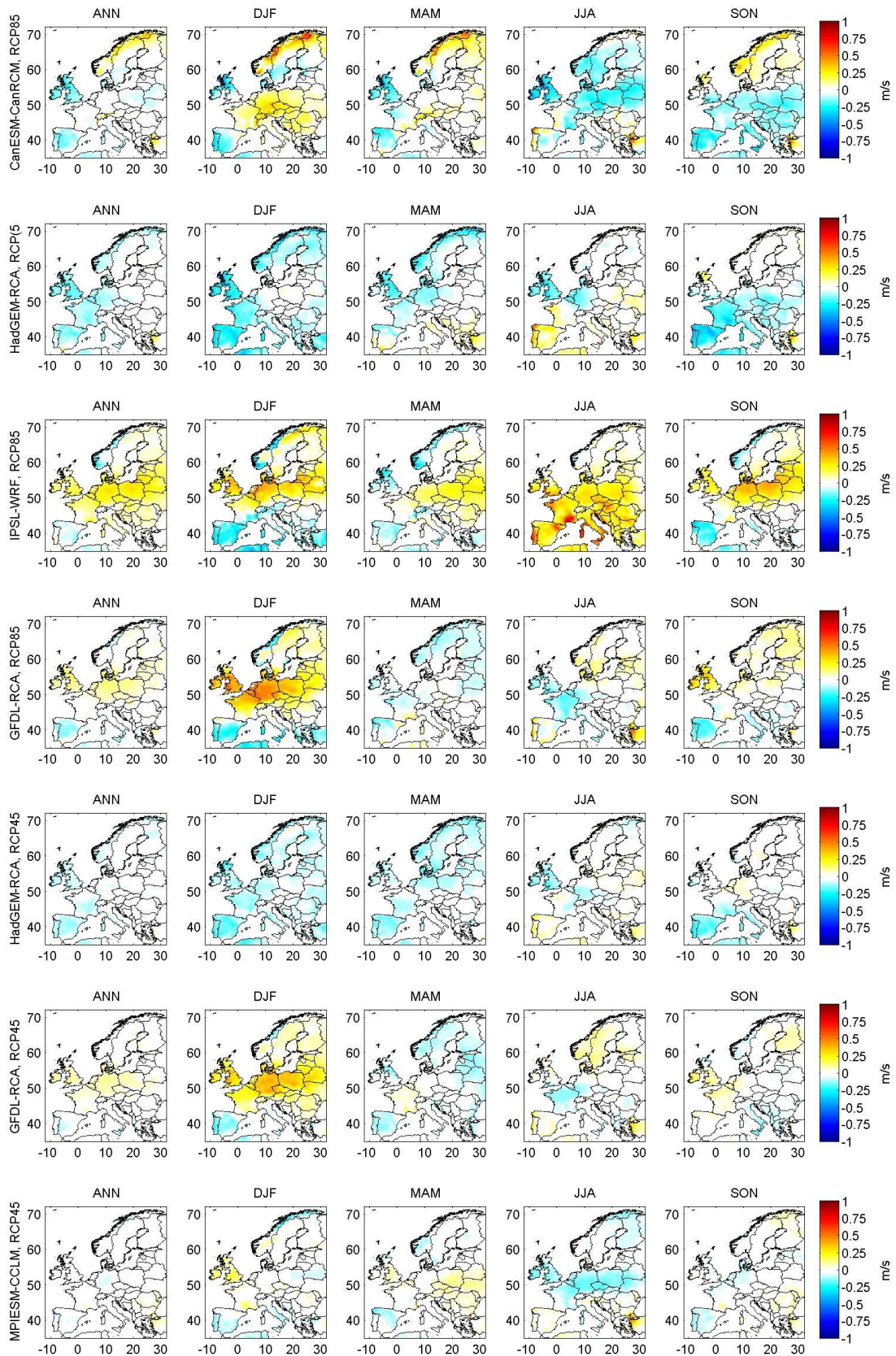


Figure 3.13: The climate change signal of short-wave radiation (2071-2100 minus 1981-2010) for all 7 models used in IMPRESSIONS illustrating model spread.



**Figure 3.14: The climate change signal of surface 10m wind speed (2071-2100 minus 1981-2010) for all 7 models used in IMPRESSIONS illustrating model spread.**

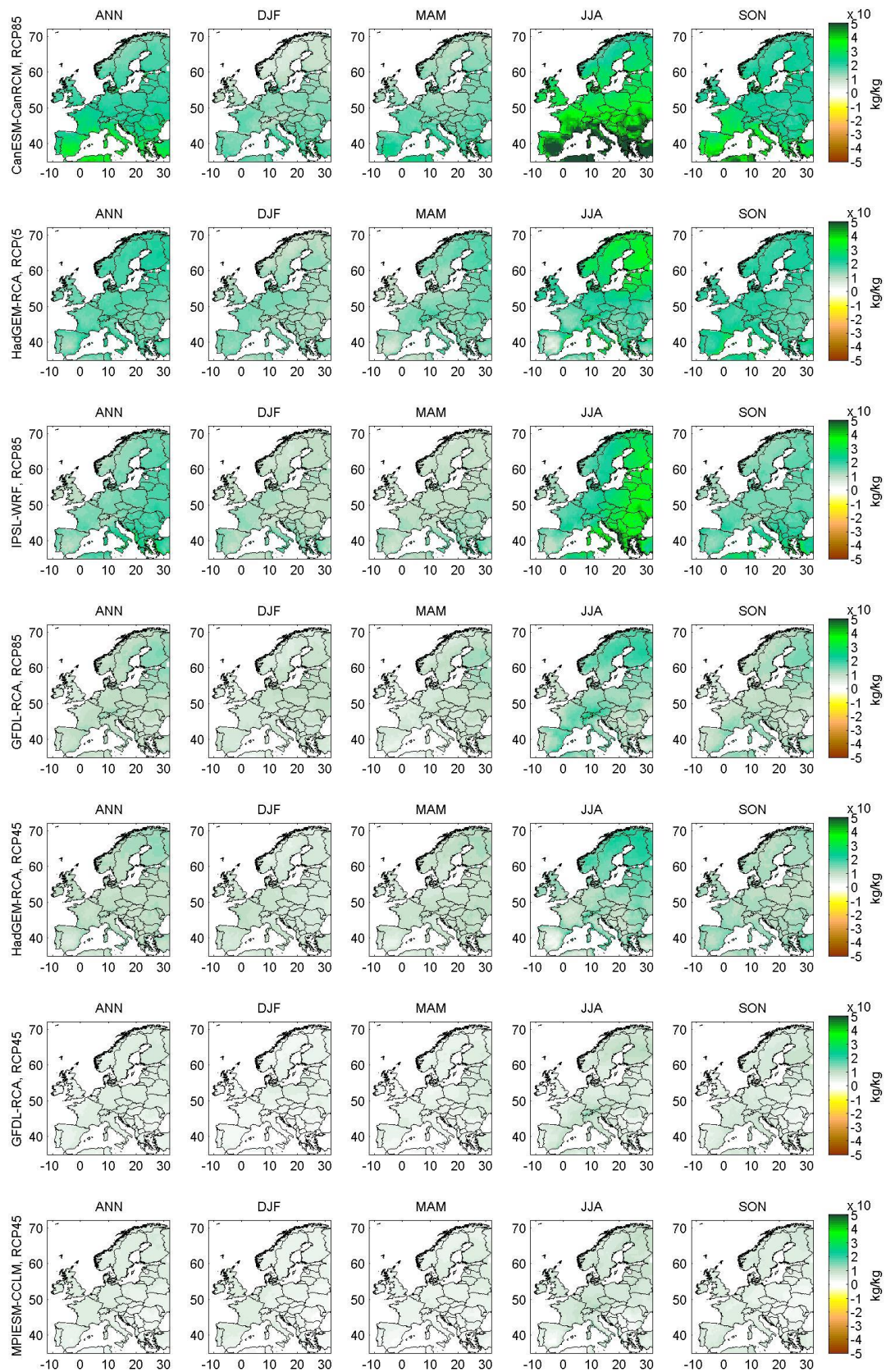
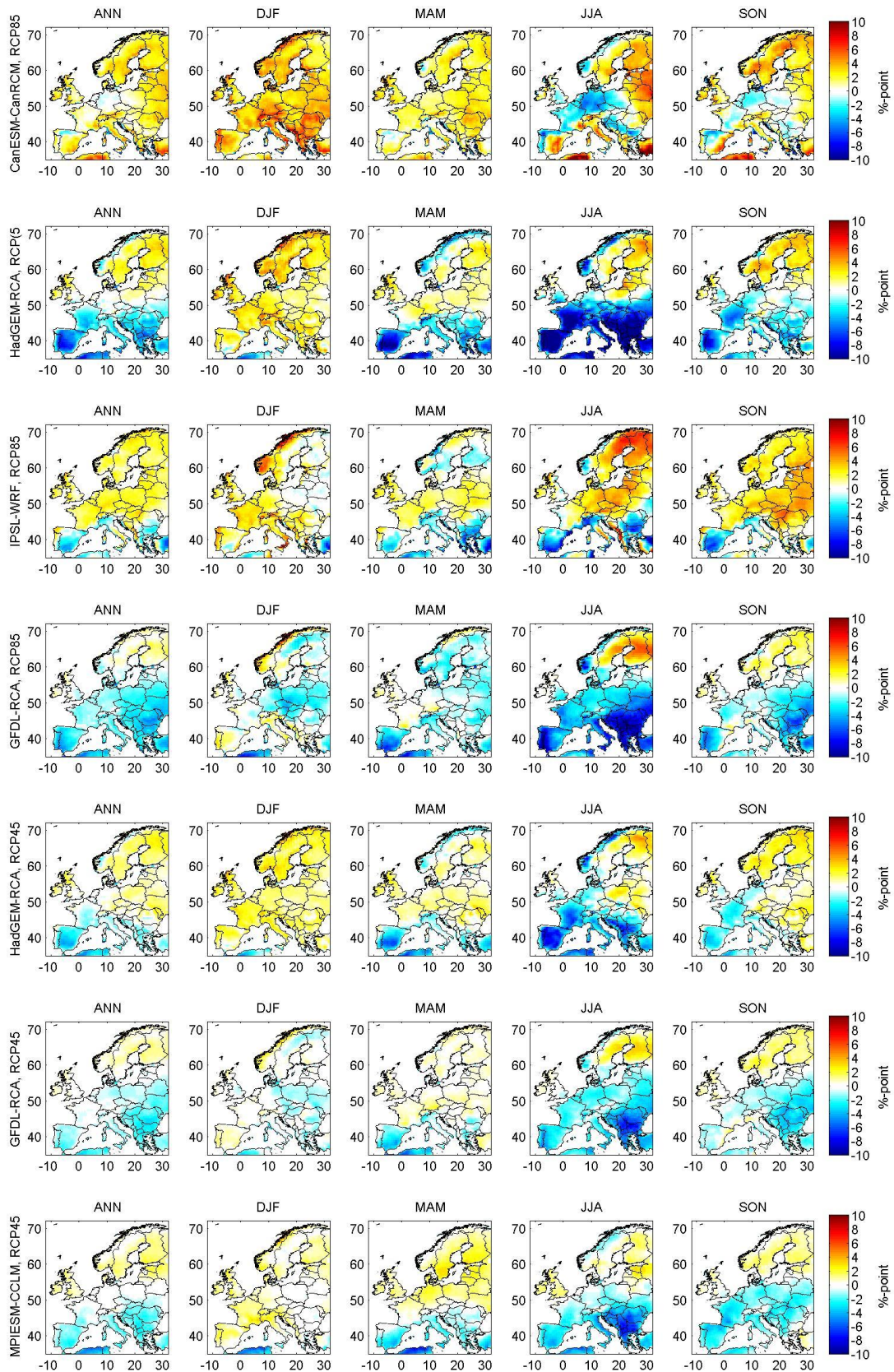


Figure 3.15: The climate change signal of specific humidity (2071-2100 minus 1981-2010) for all 7 models used in IMPRESSIONS illustrating model spread.



**Figure 3.16: The climate change signal of relative humidity (2071-2100 minus 1981-2010) for all 7 models used in IMPRESSIONS illustrating model spread.**

### 3.2. Bias-adjusted GCM data

Traditionally, the main focus of GCMs is to gain knowledge about large-scale interactions and feedbacks in the climate system. As GCMs run at relatively coarse temporal and spatial resolution, the output includes less detail in time as well as space, and most often multi-year monthly averages are used for the analysis of a GCM simulation. This means that even though daily GCM data are available, these typically compare less well with observations than the daily RCM data. That said, cases arise when there is a wish for using daily data from GCMs, most often because no or insufficient RCM data are available for the region of interest. In IMPRESSIONS, daily GCM data are used for the river catchment of Northern Dvina, Russia, as this catchment is at the edge of the European CORDEX domain. This means that there is a need for bias adjusting daily data from GCMs. In IMPRESSIONS we have chosen to use the same bias-adjustment method for GCM data as for RCM data for consistency. To our knowledge quantile mapping is not often used on GCM data, probably due to the fact the distribution of the daily data of the modelled variable need to be relatively similar to the observed distribution for quantile mapping to be successful, at least from a perspective of physical consistency. We therefore expect the bias-adjustment approach to work less effectively when daily GCM data are adjusted as compared to when daily RCM data are used.

In ISI-MIP<sup>4</sup> a quite different approach to bias-adjust daily GCM data was used. Here it was decided that the bias-adjustment technique had to conserve the climate change signal, and an ad hoc bias-adjustment procedure was built around this requirement (Hempel et al 2013). The quantile mapping procedure does not by construction conserve the climate change signal, although ideally it should not change it too much. In this section, we first present the bias-adjusted GCM data and then compare the climate change signal of GCM and RCM data before and after bias-adjustment.

In Figures 3.17 and 3.18, the 30-year seasonal mean biases of temperature, precipitation, short-wave radiation, and specific and relative humidity are shown before and after the bias-adjustment has been applied. Note that relative humidity was only available for a few GCMs and is instead derived from specific humidity using the Arden Buck equation. Also note, that we did not bias-adjust surface wind speed for the GCM data.

The bias of the direct GCM output is large in all variables (Figure 3.17), but the bias is significantly reduced after the adjustment (Figure 3.18). The bias is however still larger than the bias of the adjusted RCM data.

---

<sup>4</sup> ISI-MIP, the first Inter-Sectoral Impact Model Intercomparison Project ([www.isi-mip.org](http://www.isi-mip.org))

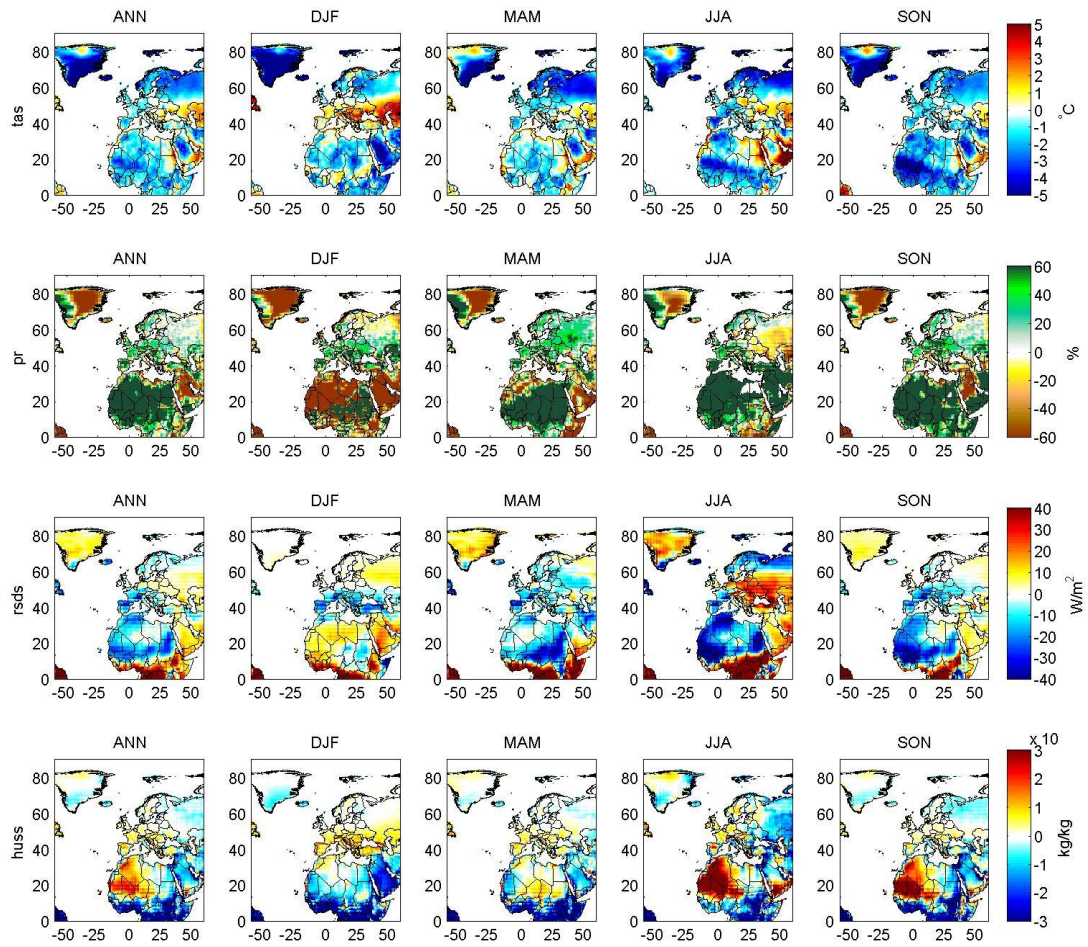
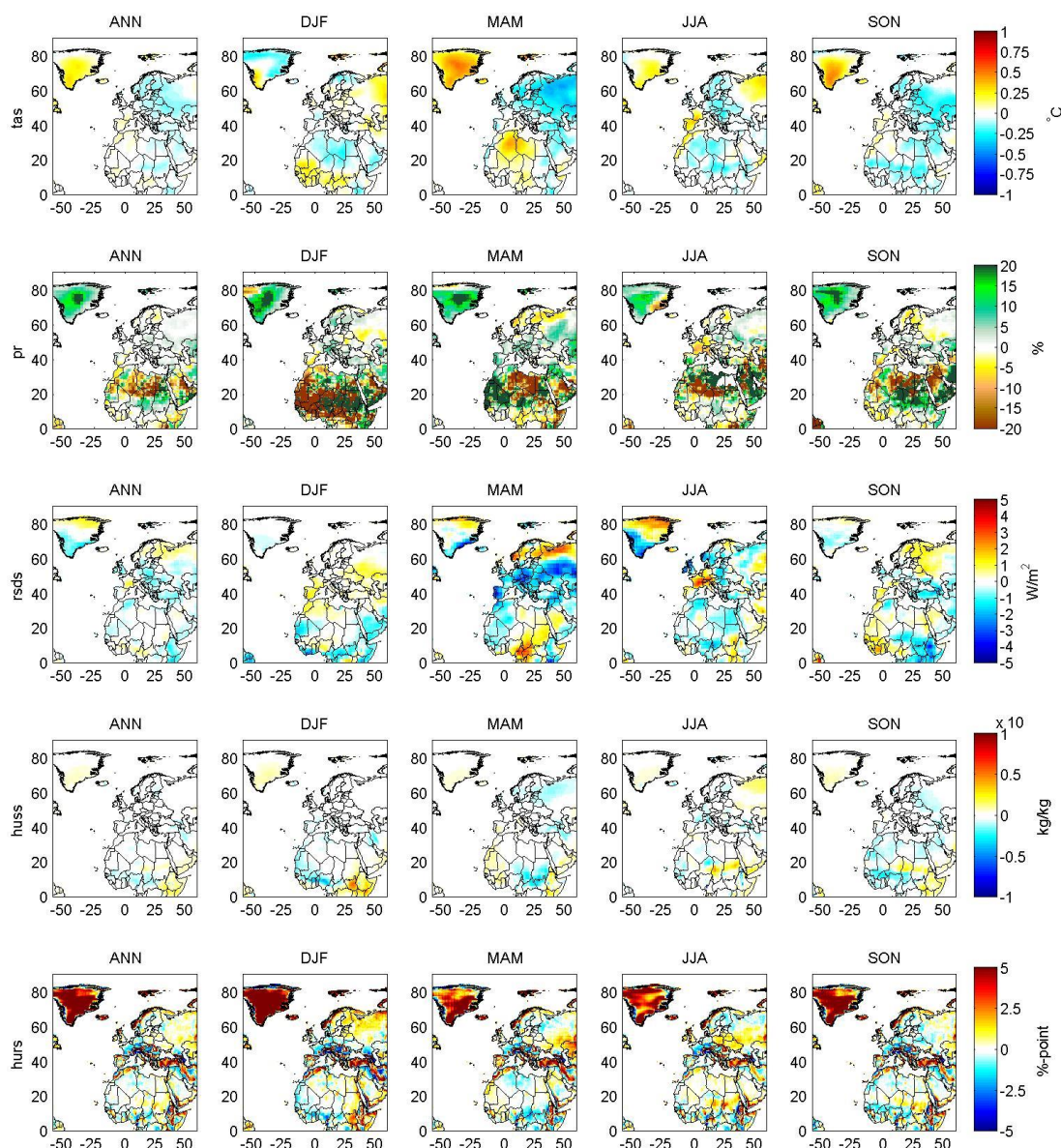


Figure 3.17: Bias of GFDL-ESM2M before bias-adjustment with regard to WFDEI 1981-2010.



**Figure 3.18: Bias of GFDL-ESM2M after bias-adjustment with regard to WFDEI 1981-2010.**

Figures 3.19-3.23 show the projected changes in temperature, precipitation, short-wave radiation, and specific and relative humidity for CanESM (RCP8.5) for all three time slices. The climate change for the European region may be compared to the climate change projected by the RCMs. Specifically, we note that the change in short-wave radiation projected by CanESM has a seasonal pattern similar to that projected by CanESM-RCA4 with a large increase in Europe during summer.

The spread in projected temperature and precipitation changes for the selected GCMs (2071-2100 vs 1981-2010) is illustrated in Figures 3.24-3.25 and can be compared with the spread projected by the RCMs (Figures 3.11-3.16).

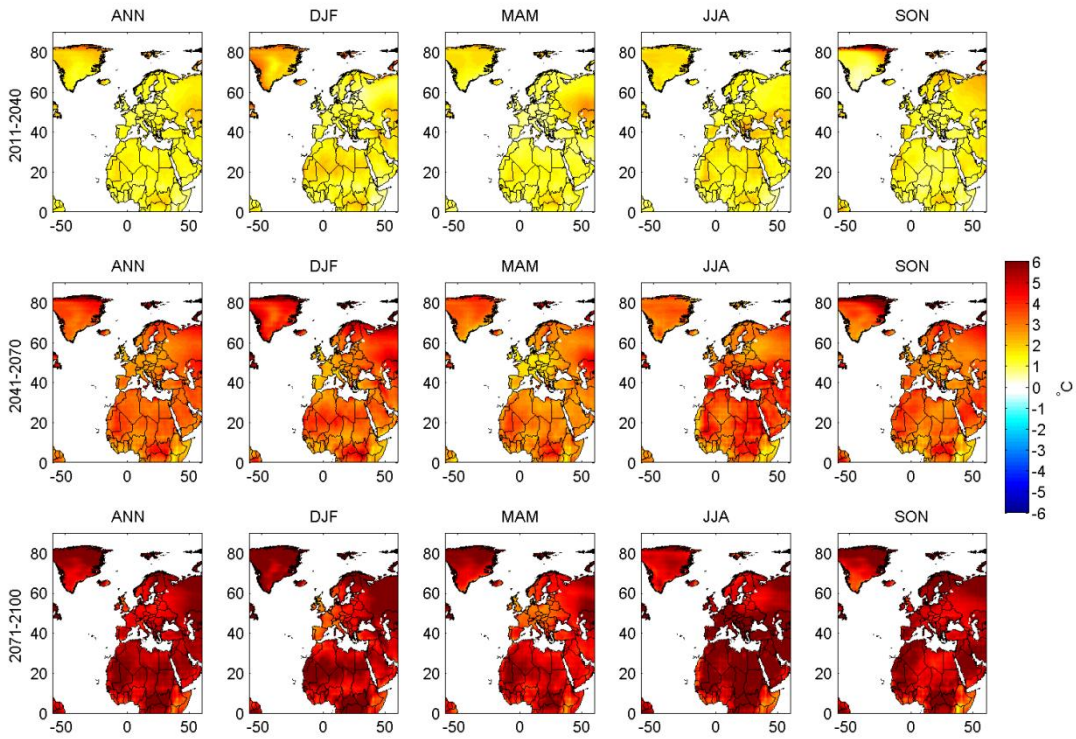


**Figure 3.19: Projected changes in temperature for CanESM – RCP8.5 with respect to 1981-2010 (bias-adjusted data).**

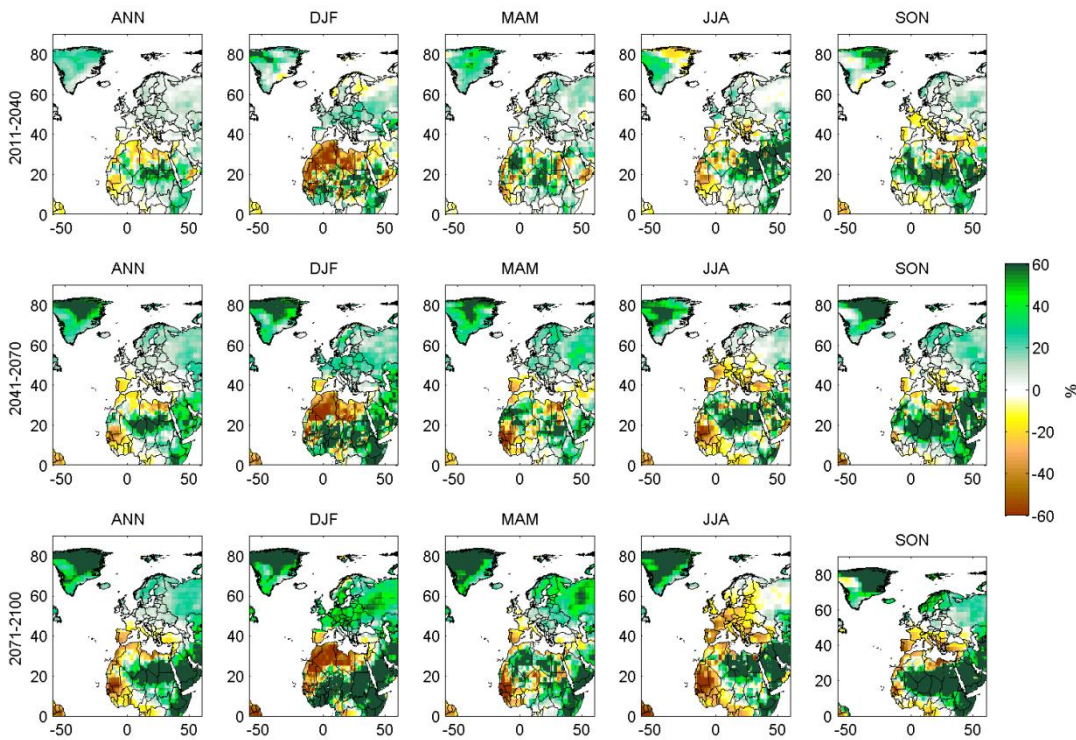


**Figure 3.20: Projected changes in precipitation for CanESM - RCP8.5 with respect to 1981-2010.**

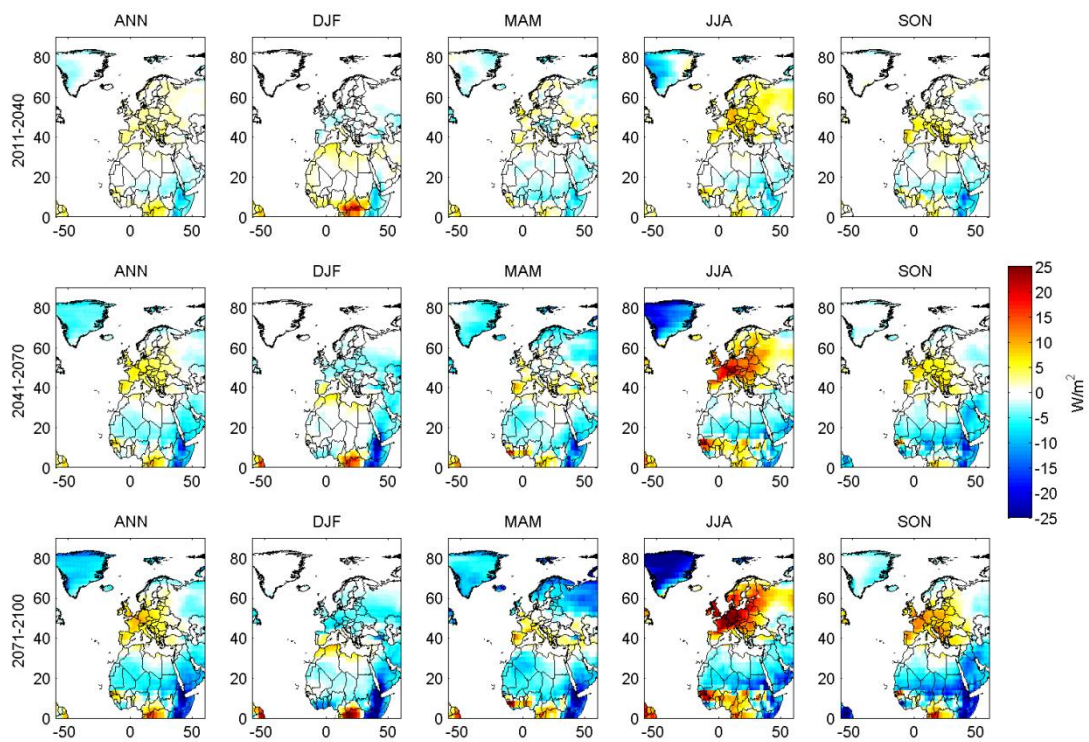


**Figure 3.21: Projected change of short-wave radiation for CanESM - RCP8.5 with respect to 1981-2010.**

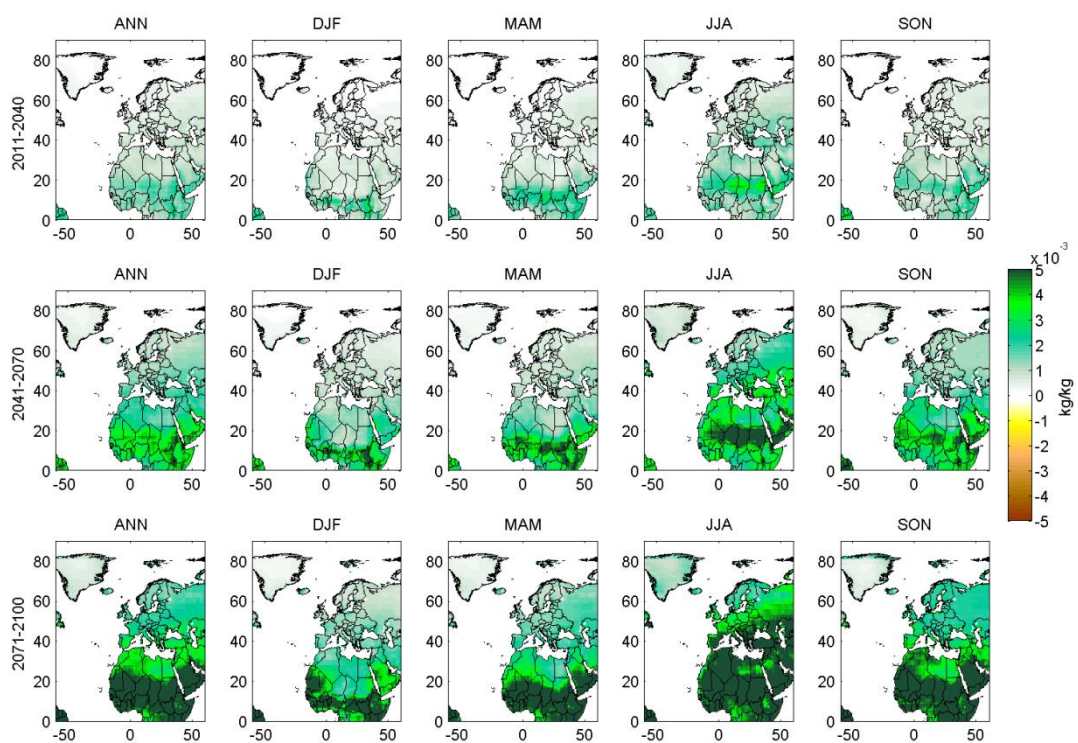


**Figure 3.22: Projected changes in specific humidity for CanESM - RCP8.5 with respect to 1981-2010.**

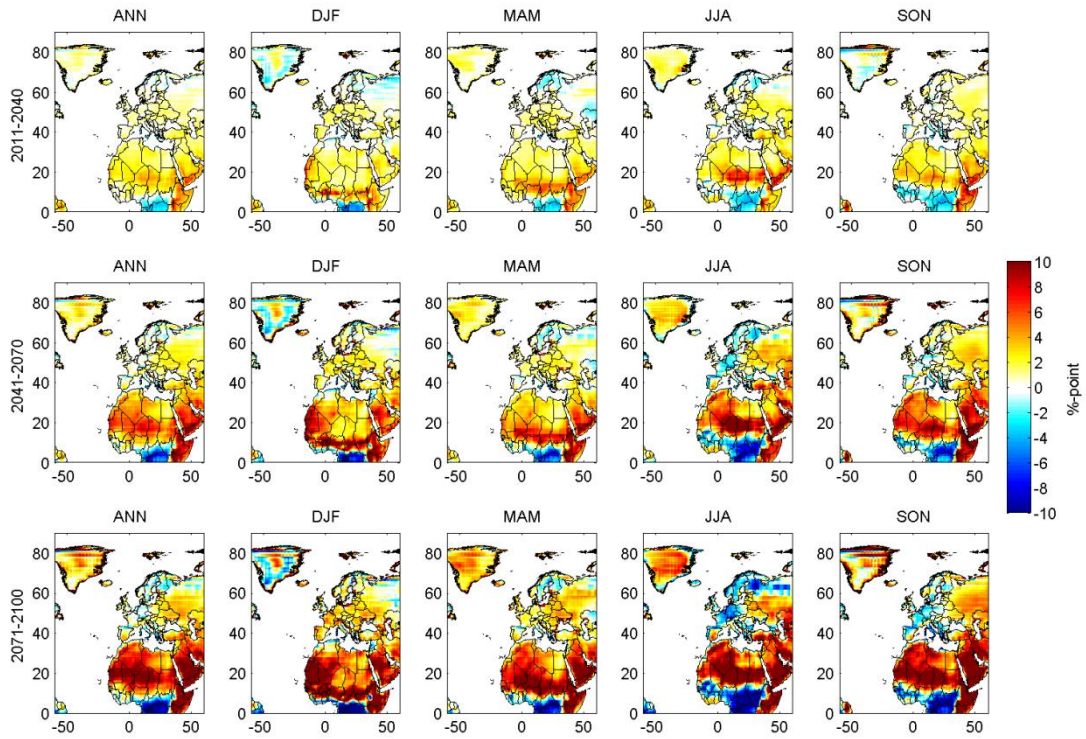


Figure 3.23: Projected change in relative humidity for CanESM - RCP8.5 with respect to 1981-2010.

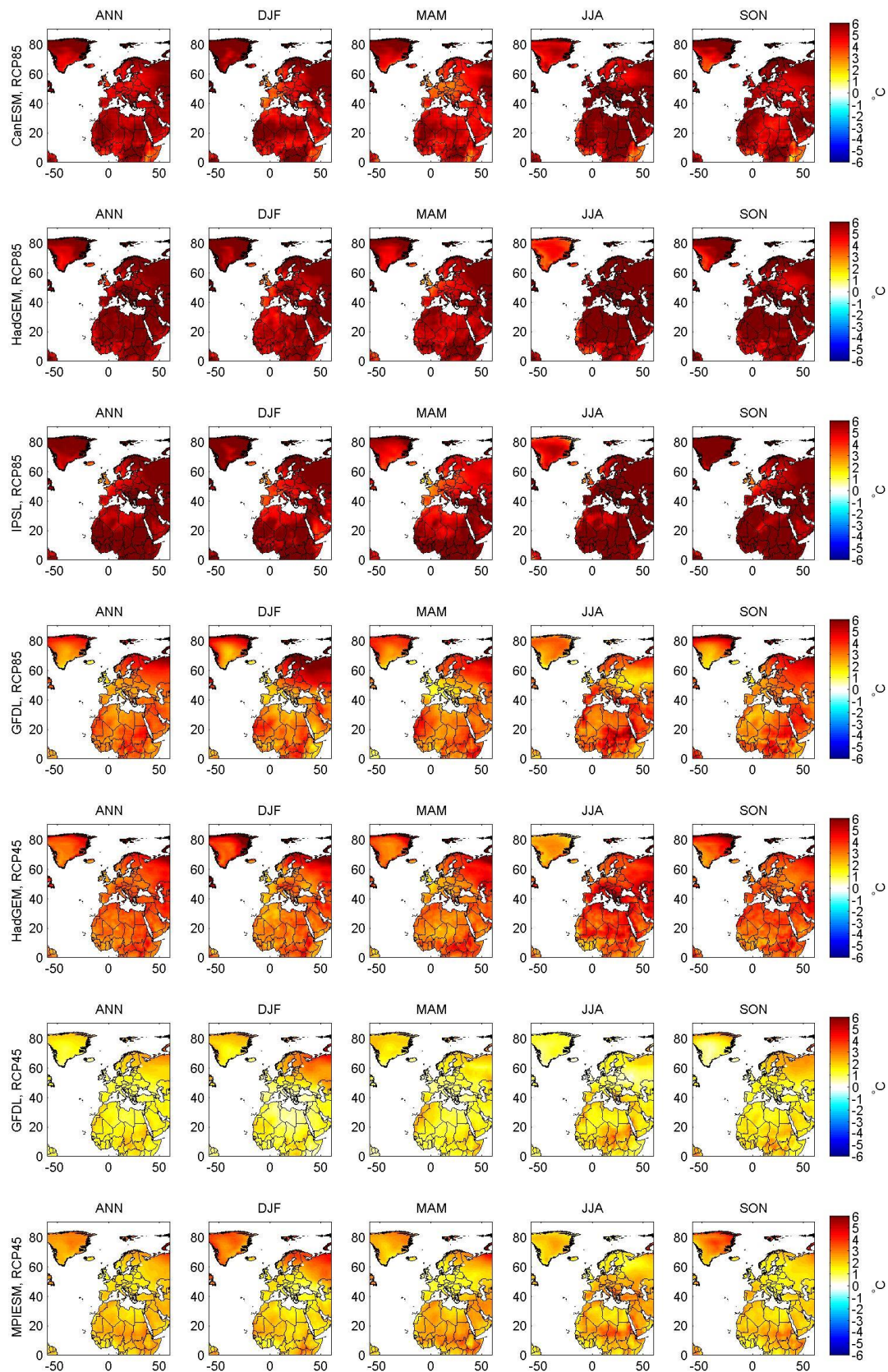
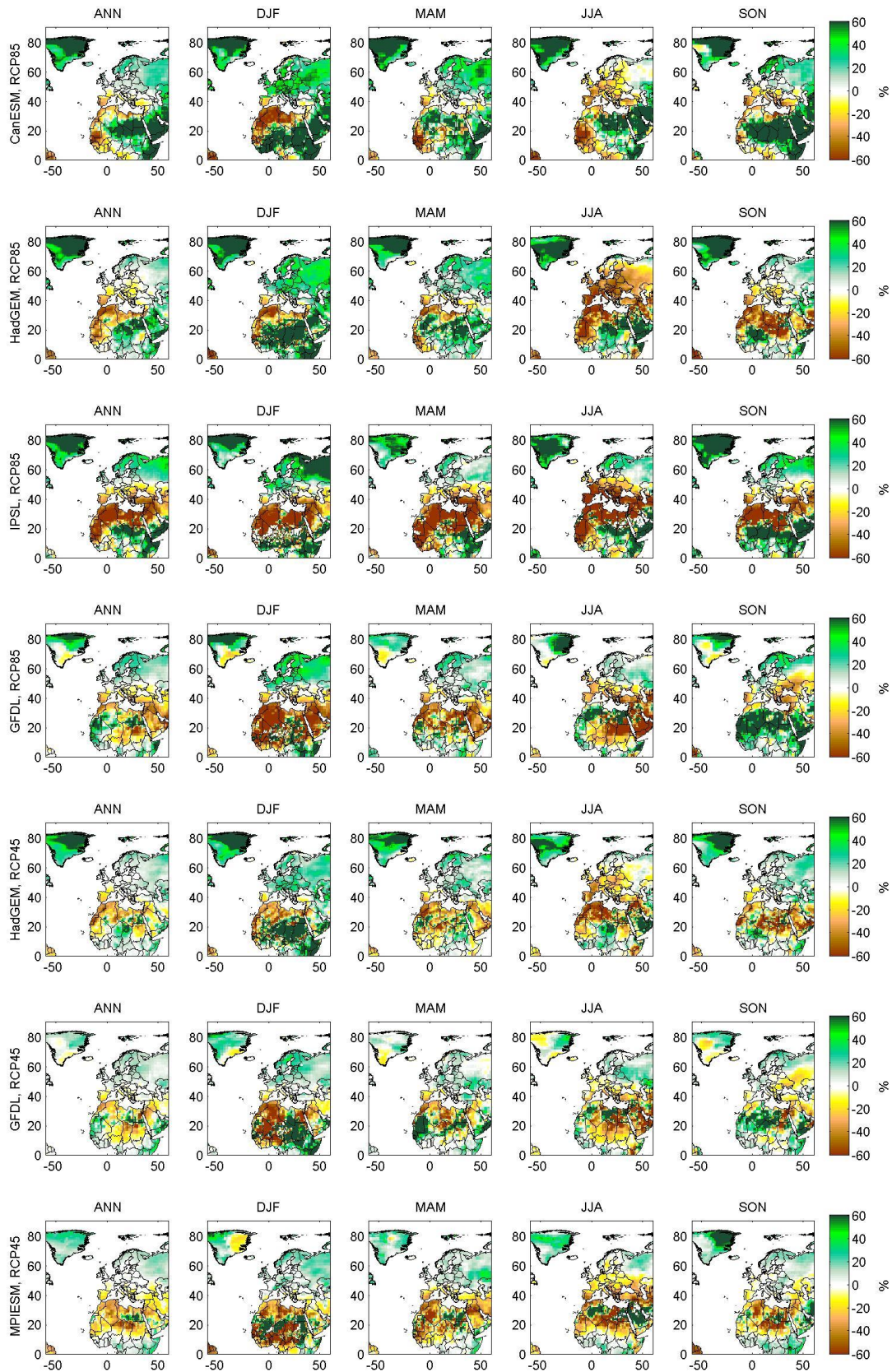


Figure 3.24: Projected temperature change for 2071-2100 for all GCM-RCM combinations.



**Figure 3.25: Projected precipitation change for 2071-2100 compared to 1981-2010 for all GCM-RCM combinations; illustrates model spread.**

### 3.3. Comparison of RCM and GCM climate change

We now have a set of GCMs each dynamically downscaled with an RCM, and both the GCM and the RCM have been bias-adjusted using the same method. The initial selection of the GCMs to be used in IMPRESSIONS was based on the change in global mean temperature (1981-2010 vs. 2071-2100) of the GCM (see Deliverable D2.1). As we consider both the GCM and the downscaling RCM in this study, we consider here to what extent the dynamical downscaling affects the climate change signal in temperature and precipitation. Figure 3.26 illustrates the climate change signal for each GCM (large symbols with black outline) and RCM (smaller filled symbols); the RCM is connected to the corresponding GCM with a line. We see that the temperature change is shifted by more than  $0.5^{\circ}\text{C}$  in some places due to the downscaling. The precipitation pattern is generally more strongly influenced by the RCM than the temperature pattern and we see larger shifts in the precipitation signal; for several GCM-RCMs the sign of the precipitation change is also shifted by the RCM (Figure 3.26).

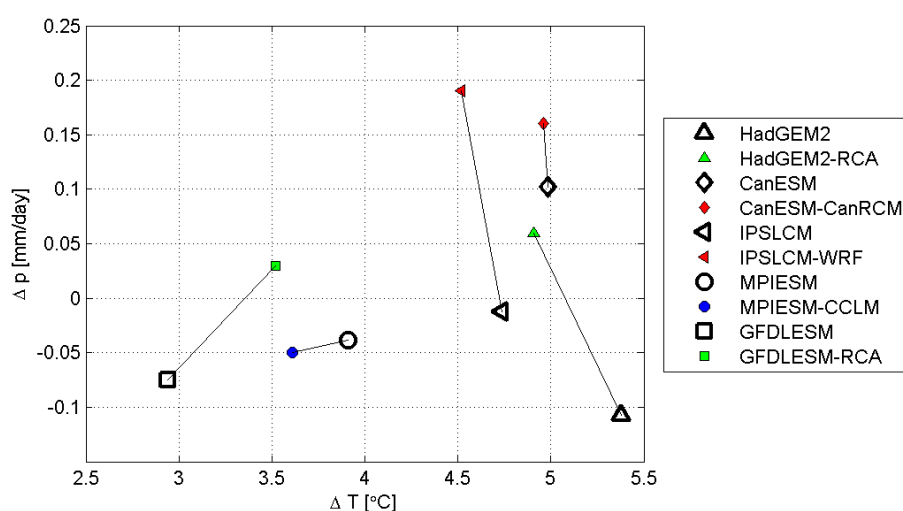


**Figure 3.26: Projected climate changes of the GCMs and their downscaled RCMs from 1981-2010 to 2071-2100. GCM represented by large symbols with black outline and RCM by smaller filled symbols.**

Figure 3.27 also compares GCM and RCM climate change signals, but here for the three local case study regions, Hungary, the British Isles (Scotland) and the Iberian Peninsula. For these, we added both the change deduced from the direct GCM-RCM output and based on the bias-adjusted GCM-RCM data; full circles indicate direct model output, open circles indicate bias-adjusted output (Figure 3.27).

It is clearly seen that the climate change signal is affected by the bias-adjustment, and for most GCM-RCM combinations, the climate change signal is affected more by the dynamical downscaling than by the bias-adjustment, but there are large local differences (Figure 3.27).

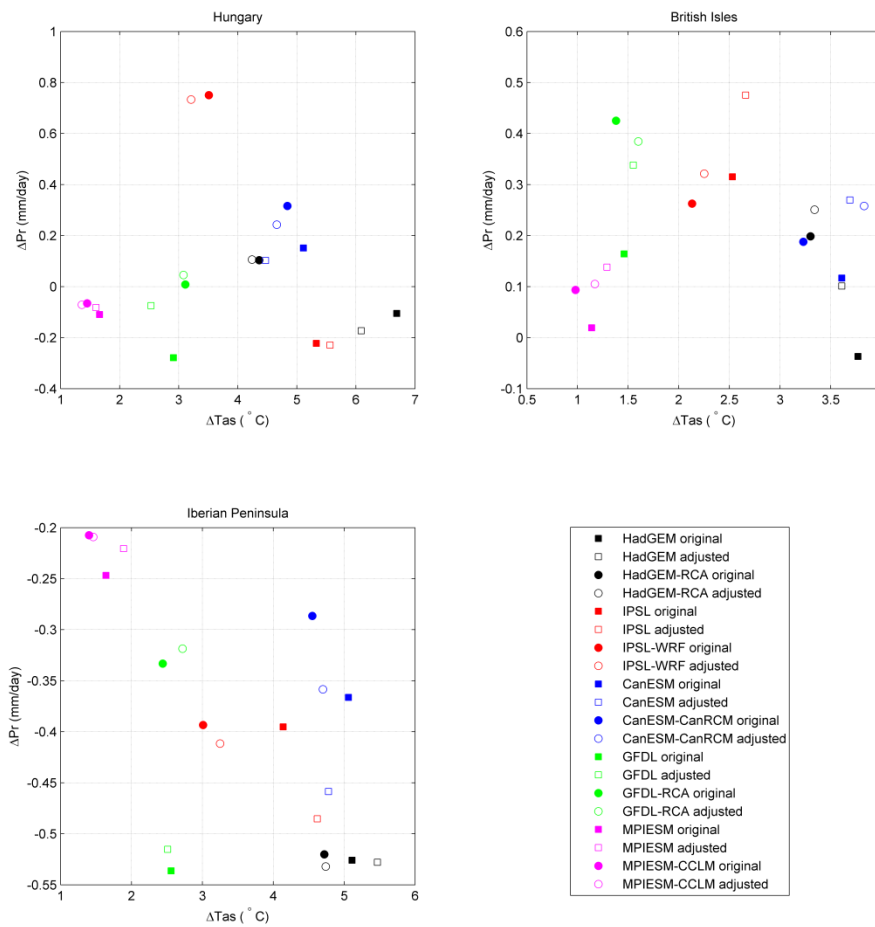


**Figure 3.27: Projected climate changes of the GCMs and their downscaled RCMs from 1981-2010 to 2071-2100 for the three IMPRESSIONS regional case study areas. Filled circles indicate direct model output, open circles indicate bias-adjusted output.**

To further look into these differences Figures 3.28-3.31 compare maps of climate change signals (1981-2010 vs 2071-2100) in summer temperature and precipitation. The upper maps in each figure are from the GCM, direct model output vs bias-adjusted and the lower maps are from the RCM. Maps to the left are based on original model output, and maps to the right are based on the bias-adjusted data. It should be stressed that the most extreme cases have been selected to illustrate that the climate change signal is significantly changed for some models/variables, while well preserved for others.

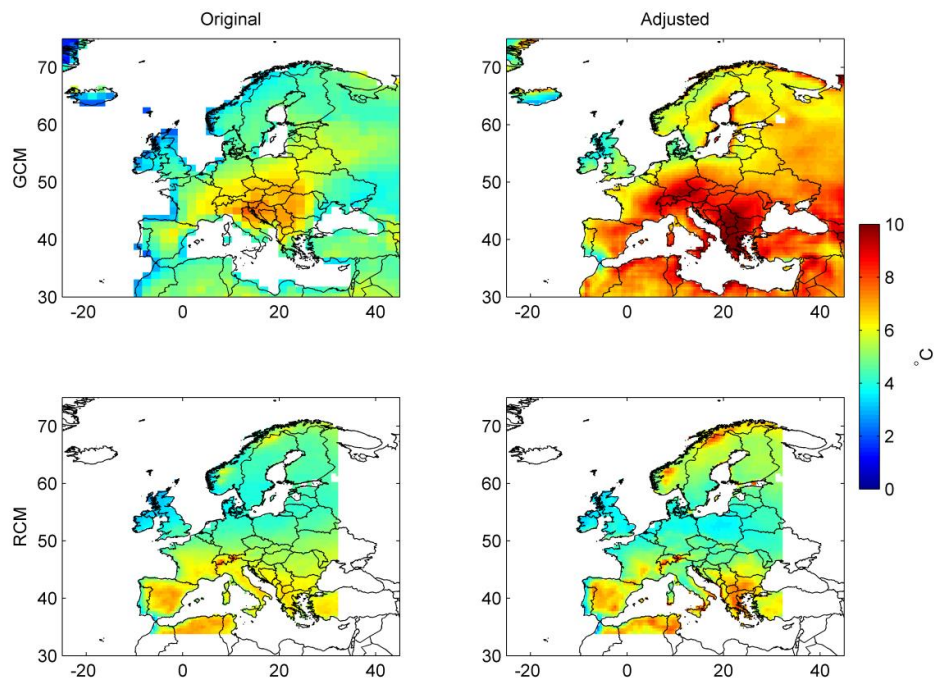


**Figure 3.28: Climate change signal in summer temperature (JJA) according to HadGEM-RCA from 1981-2010 to 2071-2100.**

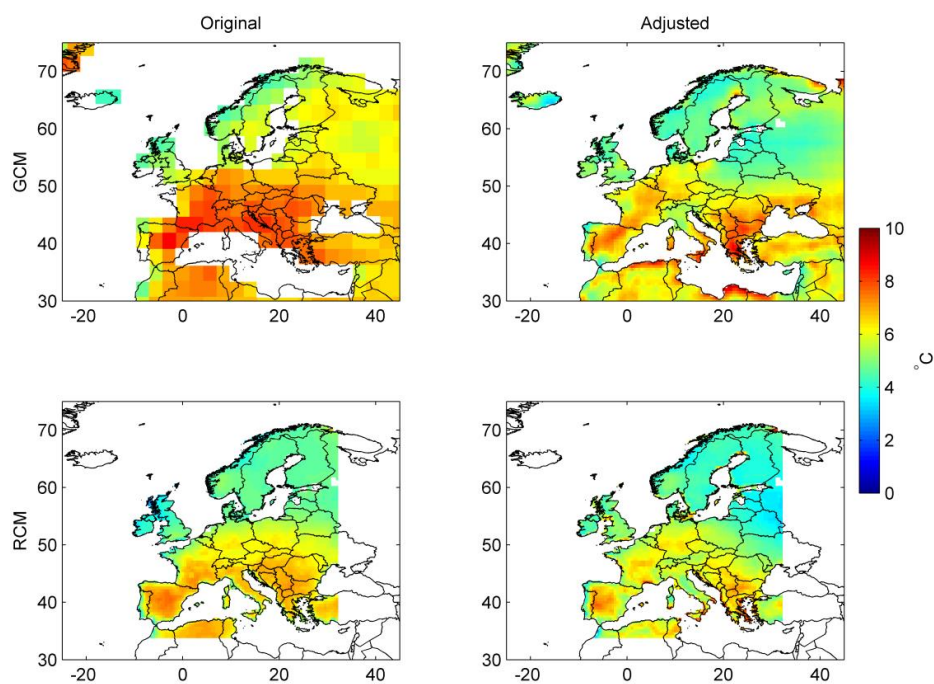


**Figure 3.29: Climate change signal in summer temperature (JJA) according to CanESM-CanRCM from 1981-2010 to 2071-2100.**

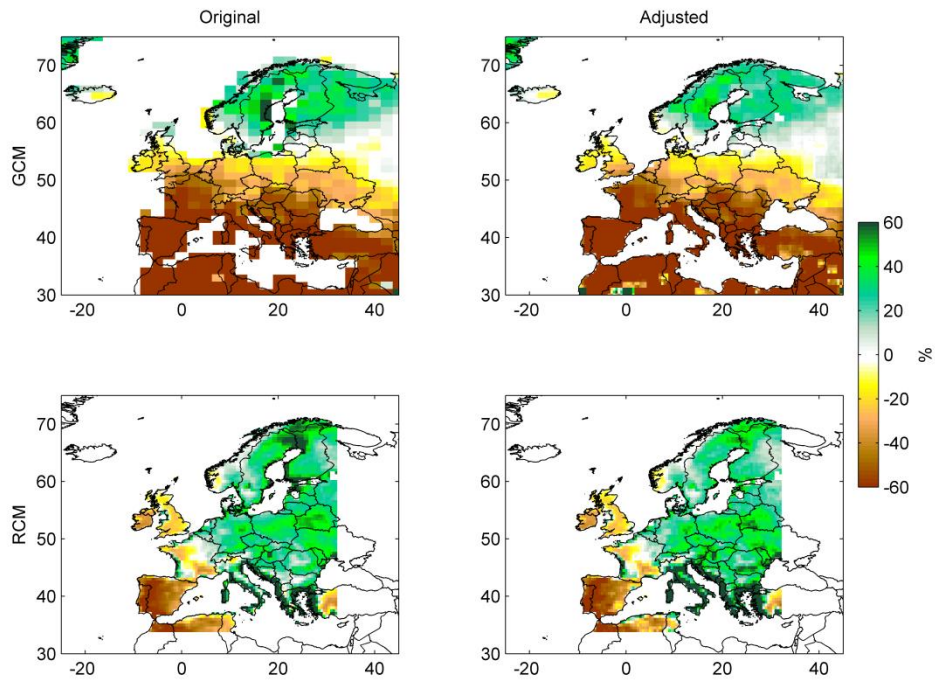


**Figure 3.30: Climate change signal in summer precipitation (JJA) according to IPSL-WRF**

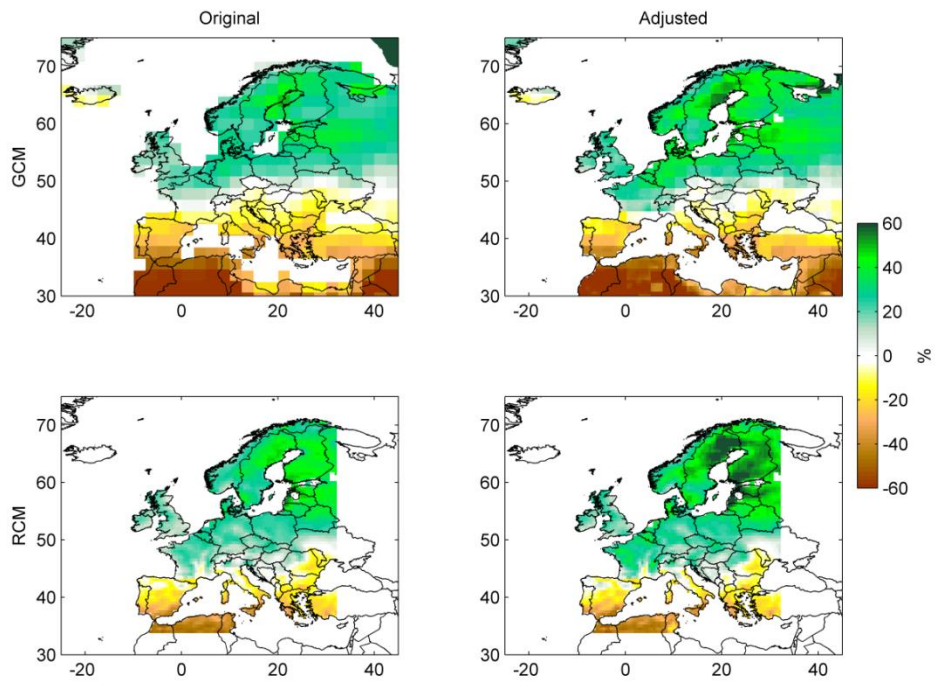


**Figure 3.31: Climate change signal in summer precipitation (JJA) according to GDFL and GFDL-RCA from 1981-2010 to 2071-2100 before and after bias-adjustment.**

For HadGEM (Figure 3.28), the climate change signal in summer temperature greatly increased following bias-adjustment. This could indicate large differences in the daily temperature distributions of HadGEM and WATCH WFDEI. The downscaling by the RCM does not change the European mean temperature change significantly but the region of largest warming is shifted from Central Europe to the Iberian Peninsula. For CanESM (Figure 3.29), the bias-adjustment has the opposite effect and actually decreases the climate change signal in summer temperature. Figures 3.30-3.31 show examples of GCM-RCMs for which the climate change signal in European summer precipitation is only slightly affected by bias-adjustment as well as dynamical downscaling.

## 4. Climate indices for Europe

A number of climate indices were calculated from the bias-adjusted daily RCM data. The most relevant indices for each local case study were selected by the impact modelers, and all indices were calculated for the whole European domain using the 0.5° resolution data. Below we have listed the indexes that are available from the IMPRESSIONS website together with the bias-adjusted data. A more detailed description of each index can be found at [http://etccdi.pacificclimate.org/list\\_27\\_indices.shtml](http://etccdi.pacificclimate.org/list_27_indices.shtml). A few selected indexes are presented below (Figures 4.1-4.4), together with several visualized products that were produced on request from the individual case studies (Figures 4.5-4.9).

### Climate indices based on temperature:

**FD**, number of frost days (days/year),

**SU25**, number of summer days with maximum temperature above 25°C (days/year),

**SU45**, number of summer days with maximum temperature above 45°C (days/year),

**TR20**, number of tropical nights with minimum temperature above 20°C (days/year),

**TN10p**, cold nights: count of days where  $T_{min} < 10$ th percentile (%),

**TX10p**, cold day-times: count of days where  $T_{max} < 10$ th percentile (%),

**TN90p**, warm nights: number of days where  $T_{min} > 90$ th percentile (%),

**TX90p**, warm day-times: count of days where  $T_{max} > 90$ th percentile (%),

**WSDI**, warm spell duration index: Annual count of days with at least 6 consecutive days where  $T_{max} > 90$ th percentile (days/year). The number of warm spell periods per year is also available,

**CSDI**, cold spell duration index: Annual count of days with at least 6 consecutive days where  $T_{min} < 10$ th percentile (days/year). The number of cold spell periods per year is also available,

**GSL**, growing season length: Annual count of days between first span of at least 6 days with daily mean temperature  $TG > 5^{\circ}C$  and first span of 6 days with  $TG < 5^{\circ}C$  (days). The start day of the growing season is also output.

### Climate indices based on precipitation:

**PRCPTOT**, Annual values of total precipitation in wet days with precipitation  $\geq 1$  mm (mm/year),

**SDII**, simple daily intensity index: The ratio of total annual precipitation on wet days to the number of wet days ( $\geq 1$ mm) (mm/day),

**R10mm**, heavy precipitation days: Annual count of days with precipitation  $\geq 10$  mm (days/year),

**R20mm**, very heavy precipitation days: Annual count of days with precipitation  $\geq 20$  mm (days/year),

**R95PTOT**, percentage of precipitation due to very wet days ( $>95$ th percentile of reference period) (%),

**CDD**, consecutive dry days: Maximum number of consecutive days with precipitation  $< 1$ mm (days/year). Annual count of the number of periods with at least 5 consecutive dry days is also available,

**CWD**, consecutive wet days: Maximum number of consecutive days with precipitation  $\geq 1$ mm (days/year). Annual count of the number of periods with at least 5 consecutive wet days is also available,

**MONsum**: Monthly values of total precipitation (mm/month),

---

**SEASsum:** Seasonal values of total precipitation (mm/season).

The number of Frost Days (FD; Figure 4.1), warm day-times (Tx90p; Figure 4.2) and Growing Season Length (GSL, Figure 4.3) are shown as examples of threshold and percentile based temperature indices. GCM-RCMs projecting high-end climate change also project the largest decrease in FD and the largest increase in Tx90p and GSL. Heavy precipitation days (R10mm; Figure 4.4) is an example of a threshold dependent precipitation index.

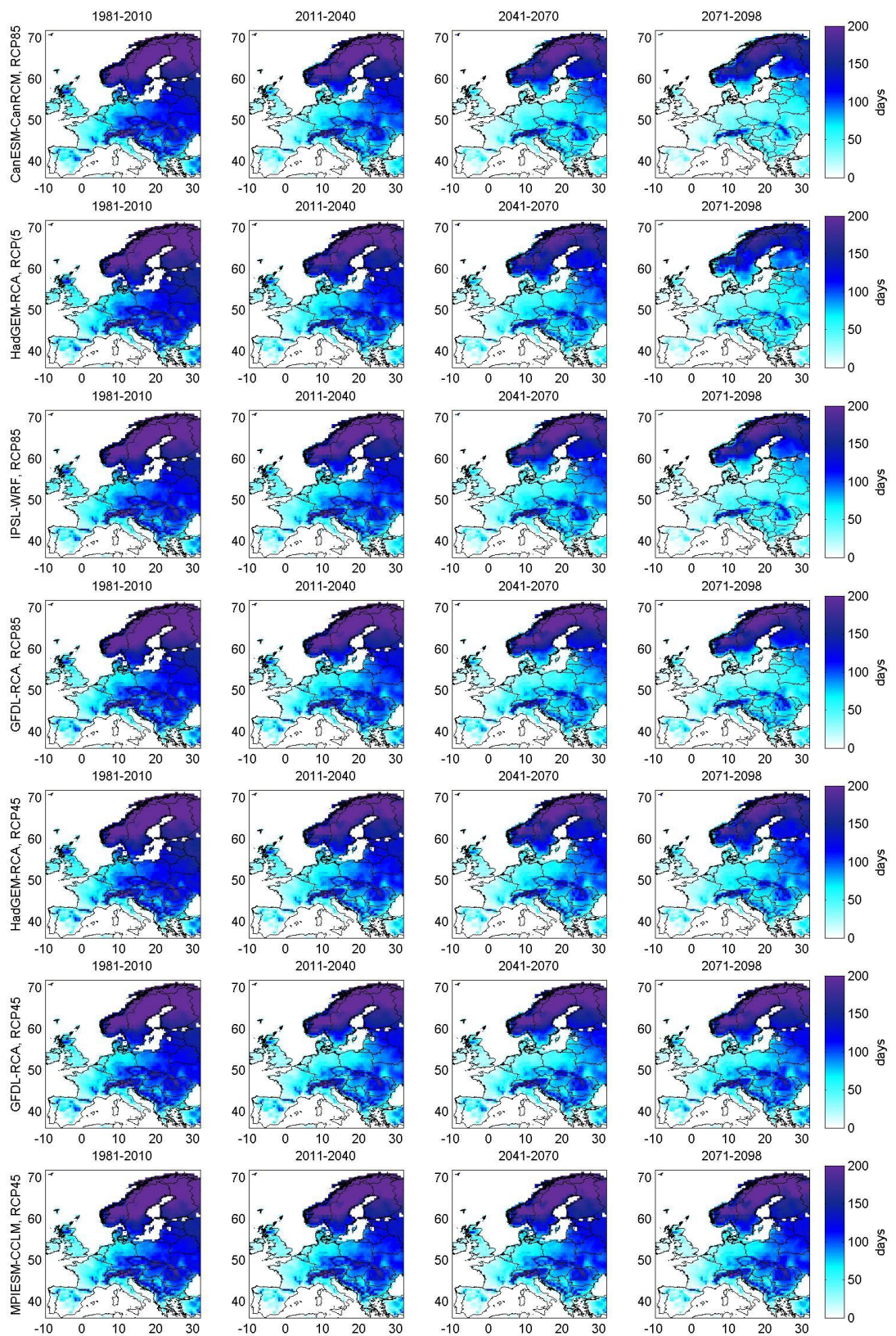


Figure 4.1: The number of frost days (FD) for all 7 GCM-RCM combinations.

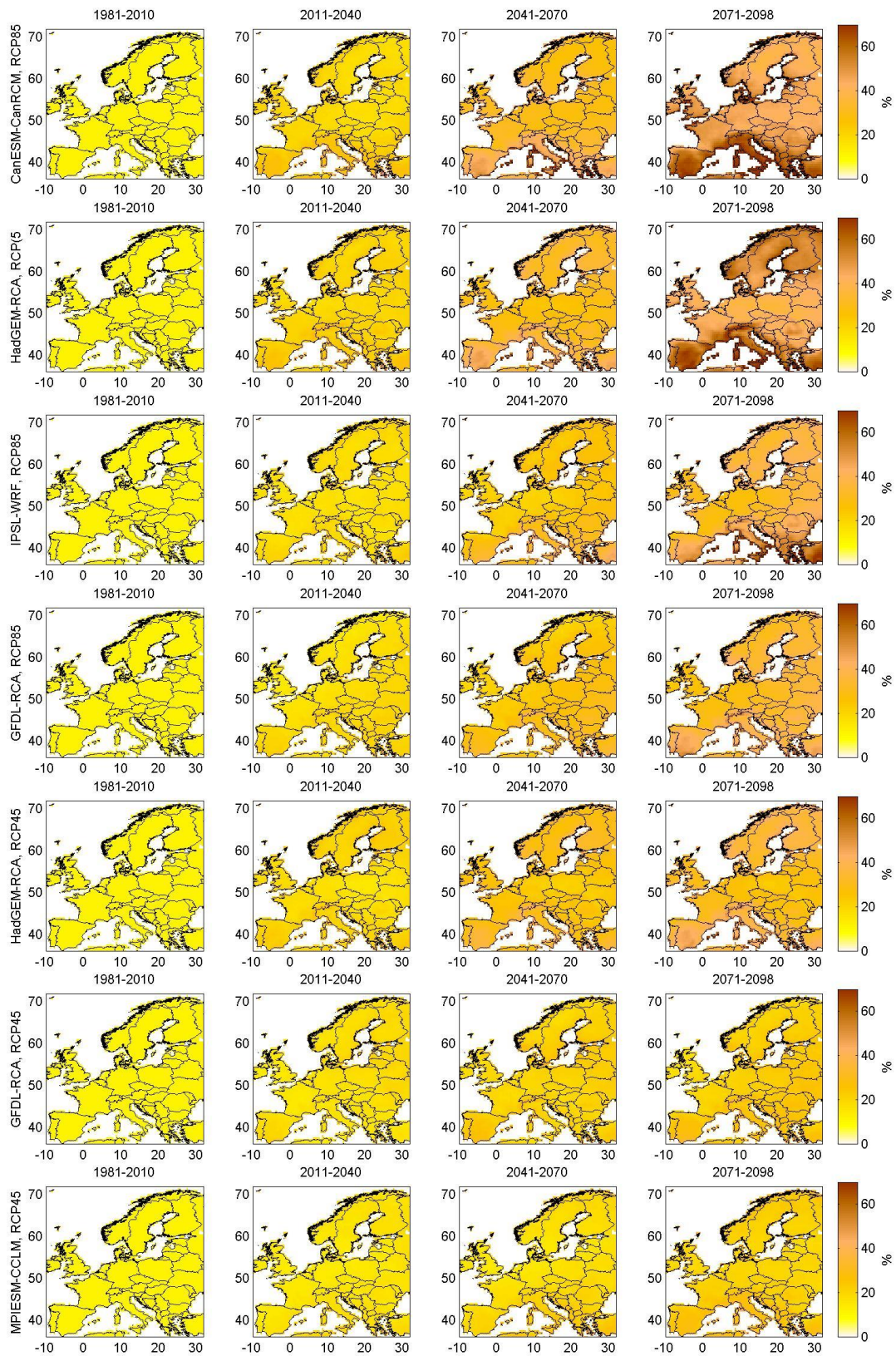


Figure 4.2: Warm day-times (TX90p) for all 7 GCM-RCM combinations.

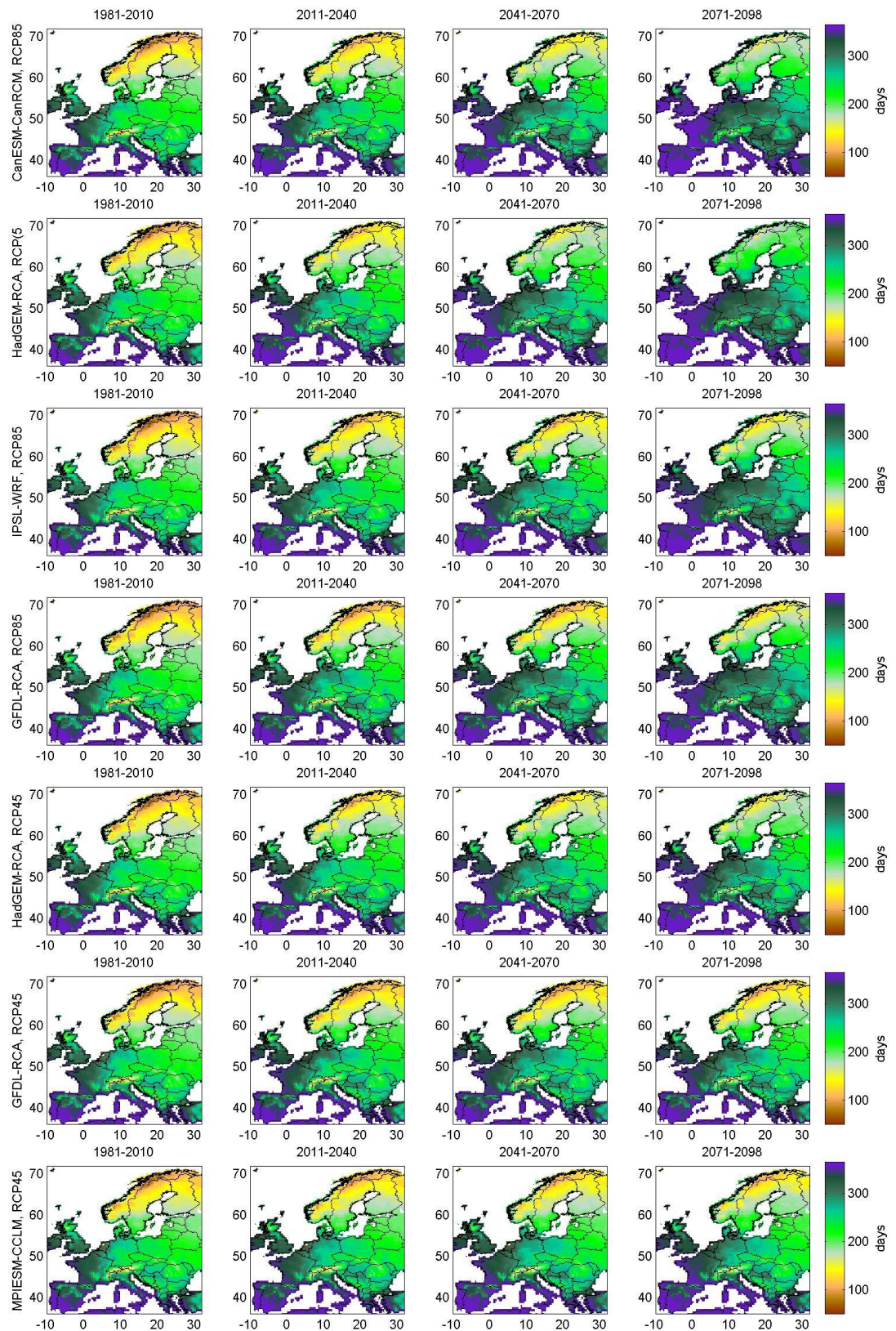


Figure 4.3: Growing season length (GSL) for all 7 GCM-RCM combinations (scale is from 50 to 365).

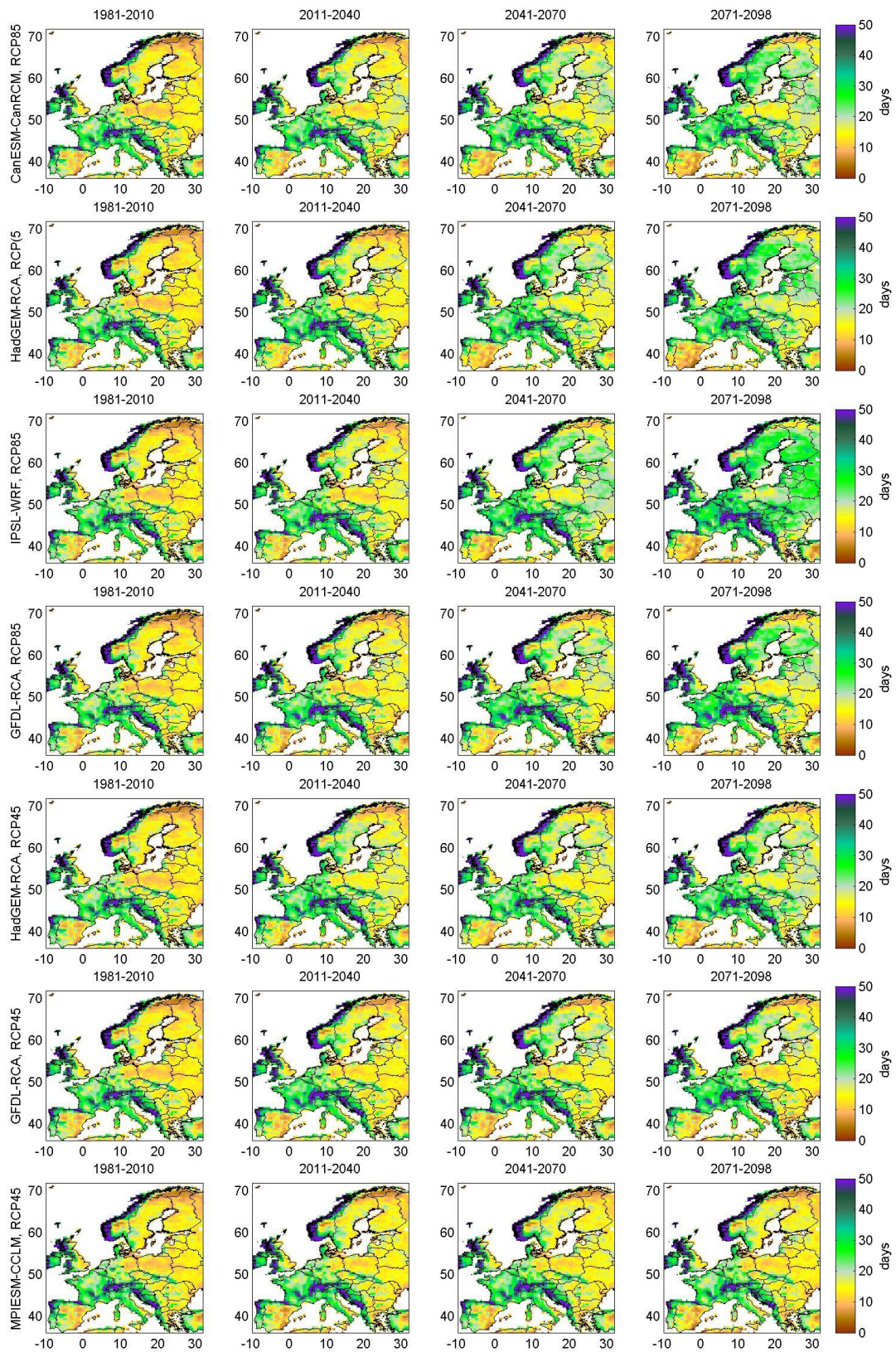


Figure 4.4: Heavy precipitation days (R10 mm) index for all 7 GCM-RCM combinations.

## 4.1. Customized data for the local case studies

A few more specific climate indices were requested by the Iberian and Hungarian case studies and these are presented below. We also show an example of one of the climate analogues that were prepared for the Scottish case study.

### 4.1.1. Standardized Precipitation Index for the Iberian case study

The Standardized Precipitation Index (SPI, McKee et al. 1993) is a normalized index representing the probability of occurrence of an observed rainfall amount when compared with the rainfall climatology at a certain geographical location over a long-term reference period. Here SPI-12 is used, as the 12-month period represents an annual evaluation of the precipitation patterns affecting large water reservoirs, such as dams and aquifers. The calibration period is naturally taken as the same as the baseline period (1981-2010). The procedure to calculate the SPI can be found here: <http://ccc.atmos.colostate.edu/pub/spi.pdf>.

Figure 4.5 shows the number of droughts according to CanESM-CanRCM (RCP8.5) for the baseline period as well as three future 30-yr time slices; it is the number of events per 30 years. Here a drought is defined as a coherent period where the monthly value of SPI is at or below -2. One event can be one month or several consecutive months where SPI-12 is equal to or less than -2. According to this climate model, the number of drought events increases over the entire Iberian peninsula throughout the 21<sup>st</sup> century (Figure 4.5).

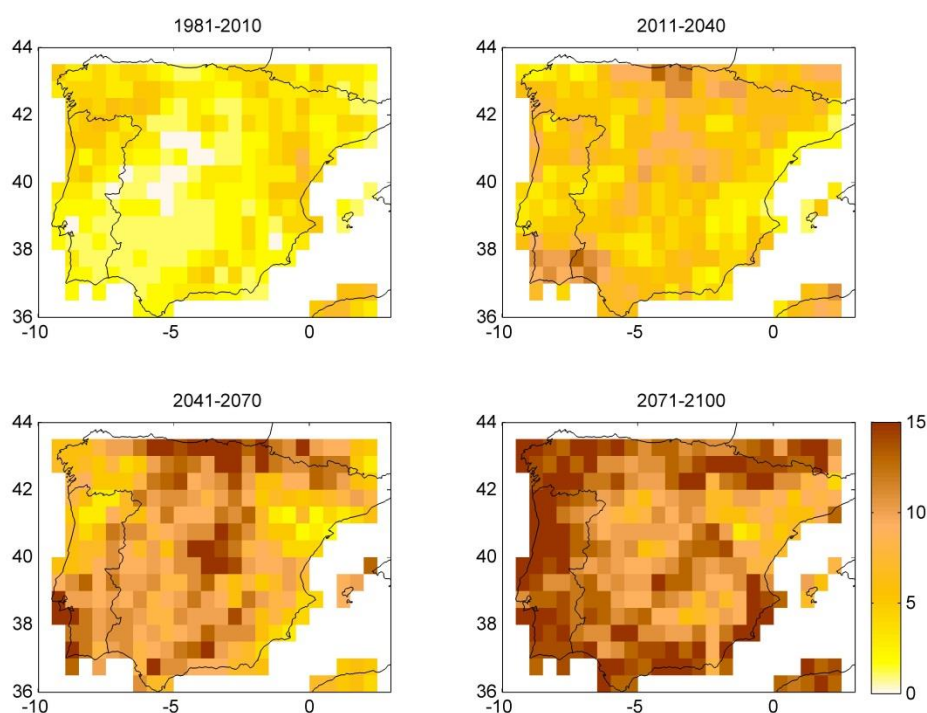


**Figure 4.5: Number of drought events over the Iberian Peninsula in each time slice based on CanESM-CanRCM4 (RCP8.5).**

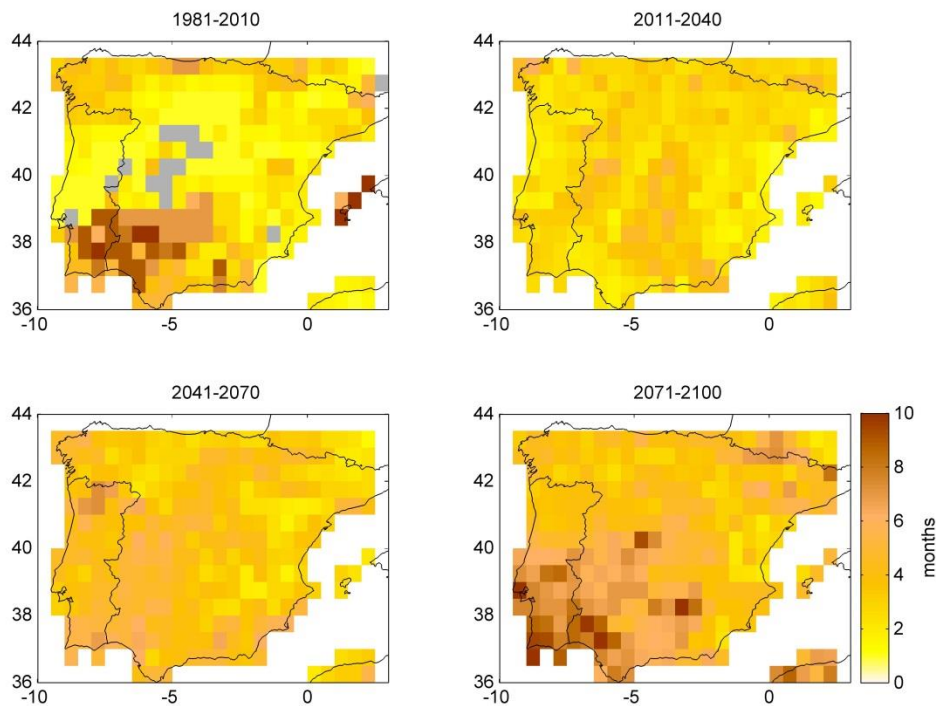


**Figure 4.6: Average duration of droughts over the Iberian Peninsula based on CanESM2-CanRCM4 (RCP8.5).**

Figure 4.6 shows the average duration of the drought events in each of the 30-yr time slices, given by the number of drought events divided by the number of months with SPI less or equal to -2. Here it is seen that for this model, the number of events do not change systematically over the Iberian Peninsula, but that there are regional differences (Figure 4.6). Comparing some of the models used in IMPRESSIONS, quite different climate change signals of number of events and drought duration were found among the core set of climate models (not shown). All the models, however, agreed that the number of months with drought (SPI  $\leq -2$ ) increased throughout the 21<sup>st</sup> century.

#### 4.1.2. Heat index for Hungary

For Hungary, two heat-related indices were calculated (the Heat Index and the Heat Warning Level system) in addition to the standard temperature indices mentioned earlier.

The Heat Index (HI) is what the temperature feels like to the human body when relative humidity is combined with the air temperature. It is an index used more in the US than in Europe, and therefore values of the Heat Index are often cited in degrees Fahrenheit. This is also the case here but it would be quite straightforward to convert values of the Heat Index into degrees Celsius. The Heat Index depends on both temperature and humidity, as both influence the human body's heat stress. Humidity influences the ability of the body to sweat and thereby get rid of excess heat. The Heat Index is built empirically and there are a multitude of different ways to calculate it. The algorithm by the U.S. National Weather Service (NWS) has been used here, as this has proven to perform well compared to other algorithms (Anderson et al., 2013). The Heat Index takes the temperature and the humidity and combines it into an apparent temperature, which relates to the heat stress felt by the body of an average human and the consequences of this. Heat indices between 80-90°F (level: Caution) can cause fatigue under prolonged exposure and/or physical activity, for heat indices between 90°F and 103°F

(level: Extreme Caution) heat stroke, heat cramps, or heat exhaustion is possible with prolonged exposure and/or physical activity, for heat indices between 103°F and 124°F (level: Danger) heat cramps or heat exhaustion is likely, and heat stroke possible with prolonged exposure and/or physical activity, and for heat indices above 125°F (level: Extreme Danger) heat stroke becomes highly likely.

Figure 4.7 shows the daily value of the Heat Index for two different 5 year periods, 1981-1985 and 2096-2100 according to CanESM-CanRCM-RCP85 (high-end model). It is clear from the figure that with the projected warming of CanESM-CanRCM that cases of Caution and Extreme Caution, which basically do not happen in the 1981-1985 period, become events that occur every summer in the period 2096-2100. More info on the Heat Index can be found here: <http://www.srh.noaa.gov/ama/?n=heatindex>.

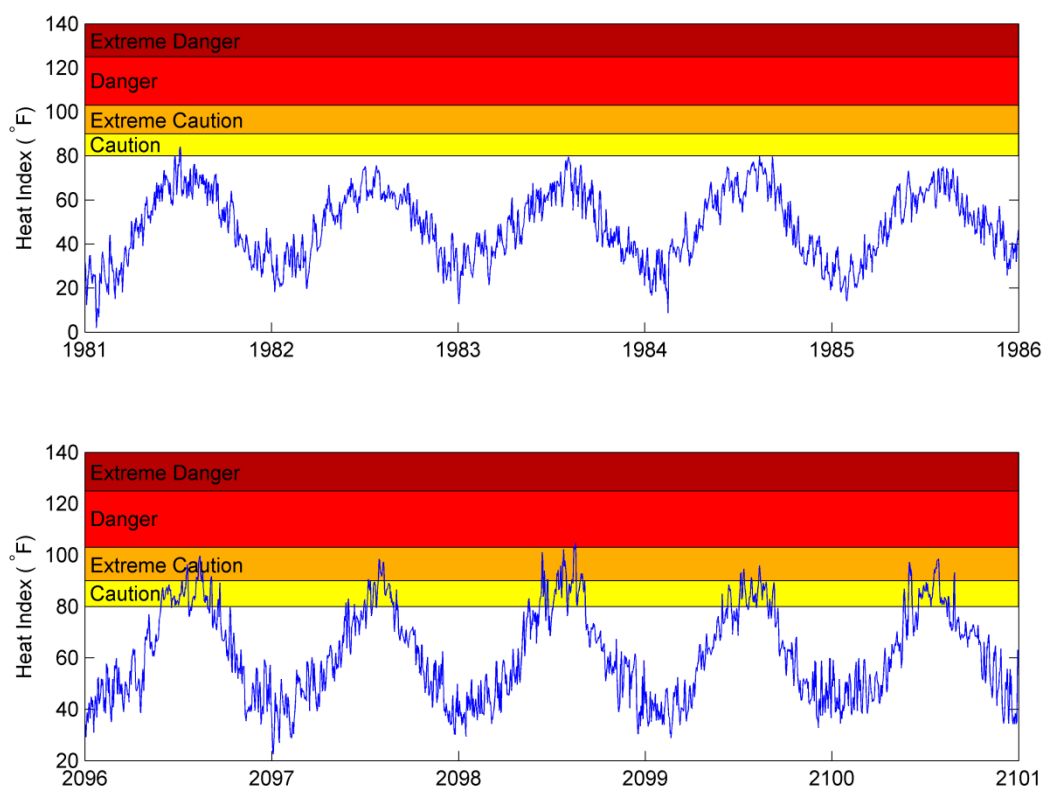


**Figure 4.7: Heat index and associated warning levels for 1981-1985 (upper) and 2096-2100 (lower) according to CanESM2-CanRCM4 RCP8.5.**

Besides the Heat Index, the heat warning level system used in Hungary was also calculated. The warning level system is a three-level warning system based on temperature thresholds as heat warning:

- 1<sup>st</sup> level of warning (for internal use): the daily mean temperature is forecasted  $\geq 25^{\circ}\text{C}$  for 1 day.
- 2<sup>nd</sup> level of warning: alert: when the Meteorological Service forecast daily mean temperature  $\geq 25^{\circ}\text{C}$  for at least 3 consecutive days.
- 3<sup>rd</sup> level of warning: alarm: when the Meteorological Service forecast daily mean temperature  $\geq 27^{\circ}\text{C}$  for at least 3 consecutive days.

This definition follows the National Public Health and Medical Office Service (ANTSZ)<sup>5</sup>, often a second criterion is included in the level 2 warning, namely that the daily mean temperature forecasted  $\geq 27^{\circ}\text{C}$  for 1 day (L: Pinter, personal communication, 2016), this was however not included here.

The different levels of warning were calculated from the daily temperature data of the regional climate models for all grid points in Hungary. Figure 4.8 shows the climate changes in the number of days with the different levels of warning taken as the mean over all the grid points in Hungary; full lines are for RCP8.5 simulations while RCP4.5 simulations are shown with dashed lines. For the level 1 warnings all scenarios follow each other relatively closely, with only slightly higher values for the RCP8.5 simulations than for the RCP4.5 simulations. For level 3 warnings however, the high-end scenarios (CanESM-CanRCM-RCP85, IPSL-WRF-RCP85 and HadGEM-RCM-RCP85) show a strong increase, whereas the low-end models (GDFL-RCA-RCP45 and MPI-ESM-CCLM-RCP45) shows a very small increase (Figure 4.8).

---

<sup>5</sup> [https://www.antsz.hu/felso\\_menu/temaink/veszelyhelyzetek/hosegriasztas/fokozat.html](https://www.antsz.hu/felso_menu/temaink/veszelyhelyzetek/hosegriasztas/fokozat.html)

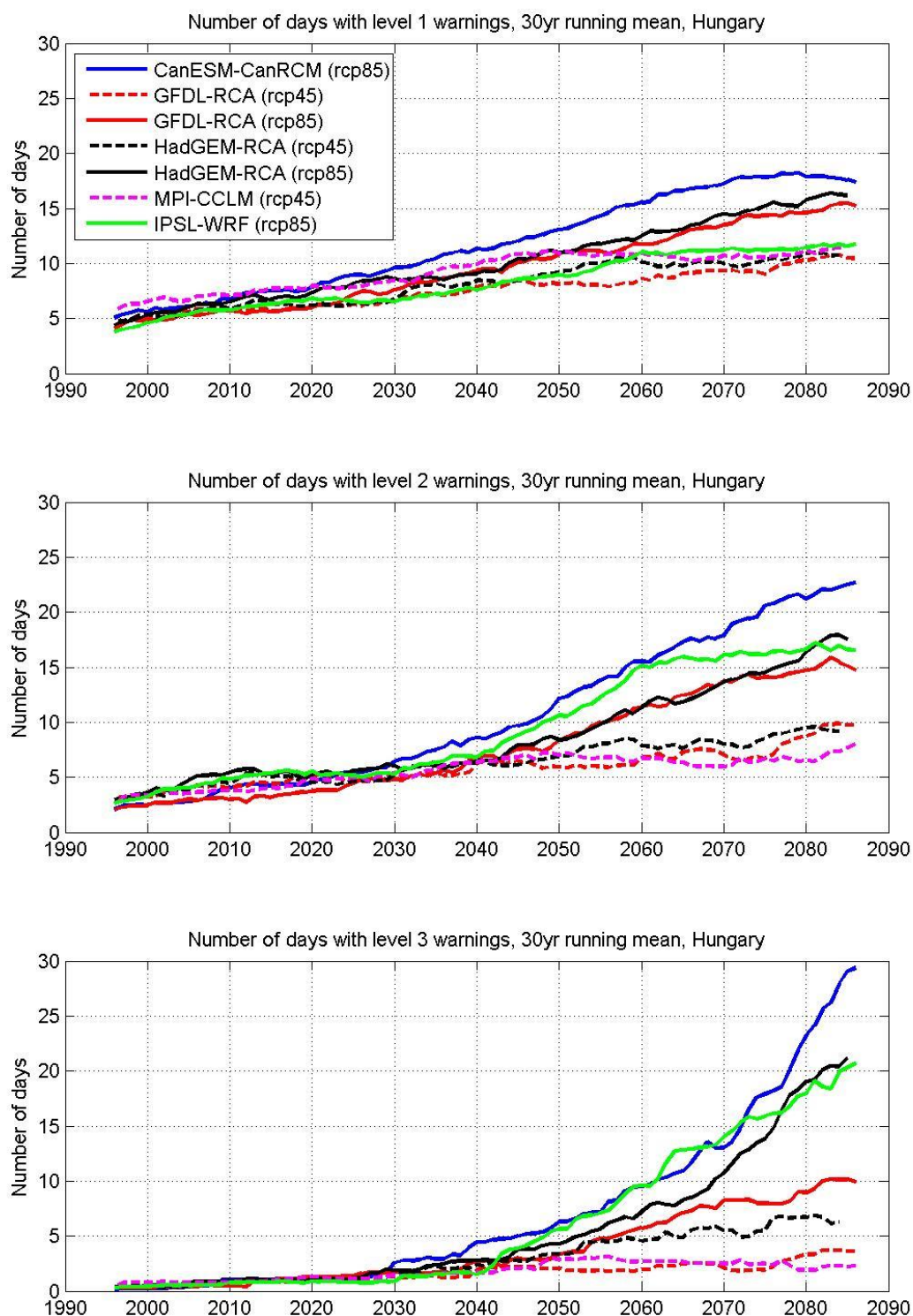
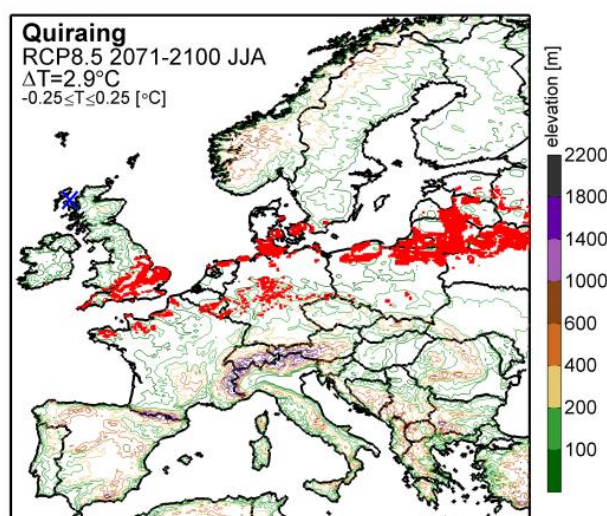


Figure 4.8: Changes in level 1, 2 and 3 heat warnings for Hungary according to the seven RCM simulations (3 RCP4.5 and 4 RCP8.5) used in IMPRESSIONS.

### 4.1.3. Climate analogues for Scotland

For Scotland, a set of climate analogues were requested to use as part of the case study work on tourism. Figure 4.9 shows an example of the climate analogue plots prepared for Scotland. The red area denotes the region which today (1981-2010) has the same annual mean temperature as Quiraing in northwest Scotland is projected to have in 2071-2100. The diagram was screened for elevation sites significantly different from the elevation of the Scottish location, so that the elevation difference is less than 300 metres at all selected (red) locations. This is because higher (or lower) elevations will tend to have quite different climate in terms of cloud and wind exposure, which will make the idea of having an analogue climate represented by one variable alone questionable. The climate analogues prepared in IMPRESSIONS were all based on the high-resolution (11km) HIRHAM simulation downscaling EC-Earth under the RCP8.5 scenario (medium climate sensitivity).



**Figure 4.9: Present-day temperature analogues for Quiraing (denoted by the blue cross) in northwest Scotland 2071-2100.**

## 5. Introduction to probabilistic climate scenarios

The scenarios described in this Deliverable are based on a sub-set of selected climate simulations and may be used to address the spread in projected climate change. However, these data are not sufficient for evaluating, for example, the risk of exceeding critical impacts, and to this end probabilistic scenarios are developed for later work in IMPRESSIONS.

The most straightforward method for determining probabilistic climate change impacts would be to use the full ensemble of climate model simulations as input for the impact models and then use the resulting ensemble of impact model results to calculate the risk of a specific impact. However, this approach is considered too demanding and therefore not often used in practice.

Another approach would be to construct an impact response surface based on a sensitivity analysis of the impact model with respect to changes in key climatic variables as suggested in Fronzek et al. (2010) and discussed in Deliverable D3.1. The risk of the impact may then be assessed by superimposing climate change projections on to the response surface. Räisänen et al. (2006) suggested increasing the sample size of climate change projections by using a simple resampling method. The main assumption

of the method is that the probability distribution of regional climate change can be related to the simulated multi-model global mean warming. As the resampled pairs correspond to a specific model output, the correlation between temperature and precipitation is restored in the resampling procedure and joint distributions of projected changes in temperature and precipitation are obtained. Using this resampling method enhances the total number of realised future climate states by the models to the degree that a density distribution function of plausible future states can be constructed, whereby a probabilistic estimate of the likely future changes can be given. The probabilistic scenarios used in IMPRESSIONS will be developed along these lines over the next six months.

A number of issues related to the selection procedure of the GCM-RCM pairs adopted in IMPRESSIONS still need further analyses in order to assess the robustness of this approach. For example, knowing to which extent the selected GCM-RCM combination actually is a fair representation of model spread still needs to be assessed. Other projects and researchers have tried to address this and their conclusions based on somewhat different methodologies needs a review in an IMPRESSIONS context (e.g. Mearns et al. 2012; Dubrovsky et al. 2015; McSweeney & Jones, 2016).

## 6. Acknowledgements

We acknowledge the World Climate Research Programme's Working Group on Regional Climate, and the Working Group on Coupled Modelling, former coordinating body of CORDEX and responsible panel for CMIP5. We also thank the climate modelling groups for producing and making available their model output. We also acknowledge the Earth System Grid Federation infrastructure an international effort led by the U.S. Department of Energy's Program for Climate Model Diagnosis and Intercomparison, the European Network for Earth System Modelling and other partners in the Global Organisation for Earth System Science Portals (GO-ESSP). We would also like to acknowledge the EU FP6 research project WATCH for data dissemination of the WFDEI data set. We thank Fredrik Boberg, DMI for preparing the climate analogue plots for Scotland.

## 7. References

- Adam, J. C. & Lettenmaier, D. P. (2003). Adjustment of global gridded precipitation for systematic bias. *J. Geophys. Res.* 108 (D9), 4257 [doi:10.1029/2002JD002499].
- Anderson, G.B., Bell, M.L. & Peng, R.D. (2013). Methods to calculate the Heat Index as an exposure metric in environmental health research. *Environmental Health perspectives*, 121, 10, 1111-1119.
- Dubrovsky, M., Trnka, M., Holman, I.P., Svobodova, E. & Harrison, P.A. (2015). Developing a reduced-form ensemble of climate change scenarios for Europe and its application to selected impact indicators. *Climatic Change*, 128, 169-186.
- Fronzek, S., Carter, T.R., Räisänen, J., Ruokolainen, L. & Luoto, M. (2010). Applying probabilistic projections of climate change with impact models: a case study for sub-arctic palsa mires in Fennoscandia. *Climate Change*, 99, 515-534.
- Harris, I., Jones, P.D., Osborn, T.J. & Lister, D.H. (2014). Updated high-resolution grids of monthly climatic observations – the CRU TS3.10 Dataset. *Int. J. Climatology*, 34, 623-642 [doi:10.1002/joc.3711].

Jones, P. W. (1999). First- and Second-Order Conservative Remapping Schemes for Grids in Spherical Coordinates. *Monthly Weather Review* 127, 2204-2210 [doi:10.1175/1520-0493(1999)127<2204:FASOCR>2.0.CO;2 (1999)].

McKee T.B., Doesken N.J. & Kleist J. (1993). The relationship of drought frequency and duration to timescales. Preprints Eighth Conf. on Applied Climatology Anaheim CA. Amer. Meteor. Soc., 179–184.

McSweeney C.F. & Jones R.G. (2016). How representative is the spread of climate projections from the 5 CMIP5 GCMs used in ISI-MIP? *Climate Services* 1 [doi: 10.1016/j.cliser.2016.02.001]

Mearns, L.O., Arritt, R., Biner, S., Bukovsky, M.S, McGinnis, S., Sain, S., Caya, D., Correia, J., Flory, D., Gutowski, W., Takle, E.S., Jones, R., Leung, R., Moufounma-Okia, W., McDaniel, L., Nunes, A-M.B., Qian, Y., Roads, J., Sloan, L. & Snyder, M. (2012). The North American regional climate change assessment program: overview of phase I results. *Bulletin of the American Meteorological Society*, 93(9), 1337-1362.

New, M., Lister, D., Hulme, M. & Makin, I. (2002). A high resolution data set of surface climate over global land areas. *Climate Research*, 21, 1-25.

Räisänen, J. & Ruokolainen, L. (2006). Probabilistic forecasts of near-term climate change based on a resampling ensemble technique. *Tellus*, 58A, 461-472.

Räty, O., Räisänen, J. & Ylhäisi, J.S. (2014). Evaluation of delta change and bias correction methods for future daily precipitation: intermodel cross-validation using ENSEMBLES simulations. *Clim. Dyn.*, 42, 2287-2303 [doi: 10.1007/s00382-014-2130-8]

Schneider, U., Becker, A., Finger, P., Meyer-Christoffer, A., Rudolf, B. & Ziese, M. (2011). GPCP Full Data Reanalysis Version 6.0 at 0.5°: Monthly Land-Surface Precipitation from Rain-Gauges built on GTS-based and Historic Data. DOI: 10.5676/DWD\_GPCP/FD\_M\_V6\_050.

Thiemeßl, M., Gobiet, A. & Heinrich, G. (2012). Empirical-statistical downscaling and error correction of regional climate models and its impact on the climate change signal, *Climatic Change*, 112, 449-468 [doi:10.1007/s10584-011-0224-4]

Weedon, G. P. Gomes, S., Viterbo, P., Shuttleworth, W. J., Blyth, E., Österle, H., Adam, J. C., Bellouin, N., Boucher, O. & Best, M. (2011). Creation of the WATCH Forcing Data and Its Use to Assess Global and Regional Reference Crop Evaporation over Land during the Twentieth Century, *J. Hydromet.* 12, 823-848 [doi:10.1175.2011JHM1369.1]

Weedon, G. P., Balsamo, G., Bellouin, N., Gomes, S., Best, M. J. & Viterbo, P. (2014). The WFDEI meteorological forcing data set: WATCH Forcing Data methodology applied to ERA-Interim reanalysis data, *Water Resour. Res.*, 50, 7505-7514 [doi:10.1002/2014WR015638]

Wilcke, R., Mendlik, T. & Gobiet, A. (2013). Multi-variable error correction of regional climate models, *Climatic Change*, 120, 871-887 [doi:10.1007/s10584-013-0845-x]